Supplemetal Information to

Epsin deficiency promotes lymphangiogenesis through regulation of VEGFR3 degradation in diabetes

Authors: Hao Wu,[1] H.N.Ashiqur Rahman,[1] Yunzhou Dong,[1] Xiaolei Liu,[2] Yang Lee,[1] Aiyun Wen,[1] Kim H. T. To,[3] Li Xiao,[8] Amy E. Birsner,[1] Lauren Bazinet,[1] Scott Wong,[1] Kai Song,[1] Megan L. Brophy,[1, 5] Md.Riaj Mahamud,[4] Baojun Chang,[7] Xiaofeng Cai,[5] Satish Pasula,[4] Sukyoung Kwak,[1] Wenxia Yang,[8] Joyce Bischoff,[1] Jian Xu,[6] Diane R. Bielenberg,[1] J. Brandon Dixon,[3] Robert J D'Amato,[1] R. Sathish Srinivasan,[4] and Hong Chen [1]*

Affiliations:
[1]Vascular Biology Program, Harvard Medical School, Boston Children's Hospital, Boston, MA 02115, USA

[2]Center for Vascular and Developmental Biology, Northwestern University Feinberg School of Medicine, Chicago, Illinois, USA

[3]Parker H. Petit Institute for Bioengineering and Bioscience, Georgia Institute of Technology, Atlanta, GA 30331, USA

[4]Cardiovascular Biology Program, Oklahoma Medical Research Foundation, Oklahoma City, OK 73104, USA

[5]Department of Biochemistry and Molecular Biology, University of Oklahoma Health Science Center, Oklahoma City, OK 73104, USA

[6]Department of Medicine, University of Oklahoma Health Science Center, Oklahoma City, OK 73104, USA

[7]Vascular Medicine Institute, Pulmonary, Allergy and Critical Care Division, University of Pittsburgh School of Medicine, Pittsburgh, PA 15261, USA

[8]Department of Nephrology, the Second Xiangya Hospital, Central South University, Changsha, Hunan, China

Running title: Epsin's role in diabetic lymphanagiogenesis

*To whom correspondence should be addressed: E-mail: hong.chen@childrens.harvard.edu; Telephone: 617-919-6304

Online-Only Extended Experimental Procedures, Supplemental Tables 1-3, Supplemental Figures 1-16.

Online-Only Extended Experimental Procedures

Antibodies, reagents and chemicals

Unless specified otherwise, common laboratory chemicals and reagents were from either Sigma-Aldrich or Fisher Scientific. Media and additives for cell culture were from Gibco. Lipofectamine 2000 transfection reagent, 5-ethynl-2'-deoxyuridine (EdU) and Alexa Fluor conjugated secondary antibodies were from Invitrogen. Oil Red O (97062-190) was from VWR. Streptozotocin (STZ), N-acetyl-L-cysteine (NAC), and Evens blue were from Sigma-Aldrich. Bovine serum albumin was from MP Biomedicals. DAF-2 was from Fisher Scientific. VEGF-C (ABIN2018451 or ABIN2003025) was from Antibodies-online.com; recombinant human VEGF-C (2179-VC) was from R&D Systems; and VEGF-C (C152S, RLT-R20-017) was from Axxora (Enzo Life Sciences). Anti-epsin 1 and anti-GAPDH (Glyceraldehyde-3-phoshate Dehydrogenase) antibodies , anti-F4/80 [Cl:A3-1] antibody, Ki-67 (M19, sc-7846) antibody, anti-VEGF-C (sc-374628) antibody, anti-LAMP-1 (sc-18821) antibody, and AP-1 (c-Jun) blocking peptide were from Santa Cruz Biotechnology Inc.; anti-epsin 2 antibody was from Columbia Biosciences; anti-VEGF-C (ab9546) antibody and rat monoclonal anti-VEGFR3 extracellular domain (ab51874) antibody were from Abcam; anti-Prox1 antibody (11-022P) was from AngioBio; GM130 mouse antibody was from Fisher Scientific, BD; anti-CD31 antibody was from BD Pharmingen; anti-CD144 (VE-cadherin) antibody was from Der-Antibody; anti-VEGFR3, anti-LYVE-1, and anti-integrin α_9 antibodies were from R&D and Cell signaling; anti-phospho-VEGFR3 antibody was from Cell Applications, Inc.; anti-phospho-AKT, anti-phospho-ERK, anti-c-Src, anti-AP-1 (c-Jun, 60A8), and anti-phospho-c-Src were from Cell Signaling Technology; anti-α-tubulin 12G10 antibody was from Developmental Studies Hybridoma Bank. Dual-Luciferase® Reporter Assay System was obtained from Promega. EpiTect® ChIP Oneday kit was purchased from QIAGEN®. The QuickChange Site-Directed Mutagenesis Kit was from Aligent. Golgi enrichment kit was purchased from Sigma-aldrich. DCFDA, cellular reactive oxygen species detection assay kit was purchased from Abcam. HDL and LDL/VLDL Cholesterol assay kit (ab65390) was from Abcam.

Animal models

Prox1-Cre-ER^{T2} mice were gifted from R. S. Srinivasan and have been described previously (1). *Epn1^{fl/fl}/Epn2^{-/-}/LYVE-1-Cre* (LEC-DKO) and *Epn1^{fl/fl}/Epn2^{-/-}/Prox1-Cre-ER^{T2}* (LEC-iDKO) mice were

generated by crossing *Epn1$^{fl/fl}$/Epn2$^{-/-}$* mice with *LYVE-1-Cre* mice or *Prox1-Cre-ER^{T2}* mice as previously described (2-4). Adult *Epn1$^{fl/fl}$/Epn2$^{-/-}$/Prox1-Cre ER^{T2}* mice on epsin 2-null background were selectively ablated of epsin 1 in LECs by administering 4-hydroxytamoxifen at 8~10 weeks old. *Epn1$^{fl/fl}$/Epn2$^{-/-}$* littermate mice without *Prox1-Cre-ER^{T2}* or wild type (WT) mice with *Prox1-Cre-ER^{T2}* were utilized as controls and denoted as WT. The mice heterozygous for VEGFR3 on an inducible LEC-specific epsins 1 and 2 deletion background (LEC-iDKO-*Flt4*$^{eGFP/+}$) were generated by crossing the LEC-iDKO mice with VEGFR3-eGFP knock-in mice (*Flt4*$^{eGFP/+}$) as described previously (4, 5). The leptin-deficient diabetic *db/db* mice (JAX^{TM} mice), were purchased from charles river.

Administration of 4-hydroxytamoxifen

The 4-hydroxytamoxifen was dissolved in DMSO at 5 mg/ml and kept at -20°C. Prior to animal administration, 4-hydroxytamoxifen was incubated at 65°C for 10 min. To obtain LEC-iDKO mice, 8-10 week-old *Epn1$^{fl/fl}$/Epn2$^{-/-}$/Prox1-Cre-ER^{T2}* mice were intraperitoneally (IP) injected with 0.3mg/30gram body weight of 4-hydroxytamoxifen using a 27-gauge needle. Treatment is continuously administered every other day for a total of 5 injections. Epsin deletion was determined by western blot analysis of primary lymphatic ECs isolated one week after the last 4-hydroxytamoxifen injection.

STZ-induced diabetes

To generate the WT/STZ/HFD and LEC-iDKO/STZ/HFD mouse models, 10~12 week-old WT and LEC-iDKO mice were injected IP with 50 mg/kg streptozotocin (STZ) for 5 consecutive days as described previously (6-8). Once hyperglycemia was induced (glucose levels reached >300 mg/dL), mice were fed high fat diet (HFD, Research Diets, Inc., Fisher) for 8-12 weeks to maintain type 2 diabetic conditions.

qRT-PCR

Total RNA of LECs isolated from WT, LEC-iDKO, WT/STZ/HFD and LEC-iDKO/STZ/HFD or LECs isolated from diabetic paitents and non-diabetic controls were extracted by using commercially available kits (Qiagen, Valencia, CA, USA) followed by DNase I treatment or TRIzol (Invitrogen), acording to

the manufacturer's instuctions. The extracted RNA was then reverse-transcribed into cDNA by using Oligo(dT)20 primers (Invitrogen-18418-020) and was subjected to qRT-PCR amplification, all primers sequence for PCR were purchased from Harvard Primer Bank (Boston, USA). PCR were performed in triplicate with the StepOnePlus Real-time PCR system (Applied Biosystems, Foster City, CA, USA) and Platinum SYBR Green qPCR super mix (Invitrogen) and Assays-on-Demand Gene Expression probes (Applied Biosyems). The average threshold cycles (Ct) of the duplicates were used to compare the relative aboundance of the mRNA. The Ct of β-actin RNA was used to normalize all samples. The qRT-PCR primer sequences for mouse LECs: epsin 1 (sense, 5'-AGATCAAGGTTCGAGAGGCAA-3', antisense, 5'-GTGAGGTCGGCAATCTCTGA-3); epsin 2 (sense, 5'-ACATCCCAGGTTTTAGGCCG-3', antisense 5'-GGAGTTTGTGGTGGGGAGAG-3'); and β-actin (sense, 5'-AGAGCTACGAGCTGCCTGAC-3', antisense, 5'-AGCACTGTGTTGGCGTACAG-3'). The qRT-PCR primer sequences for human LECs: epsin 1 (sense, 5′-GAGAGCAAGAGGGAGACTGG-3′, antisense, 5′-GTGAAGACGTCAGCAAGGTC-3′); epsin 2 (sense, 5′-CAGTCCCTCAACCCTTTCCT-3′, antisense, 5′-CGAAGCTGGTTCAGTGTCAG-3′); and β-actin (sense, 5′-AGCTGCTTCTGCGGCTCTAT-3′, antisense, 5′-GTGGACAGTGAGGCCAGGAT-3′).

Bioinformatics assay

AP-1 binding sequences on human and mouse epsins 1 and 2 promoter region from QIGEN database: http://www.sabiosciences.com/chipqpcrsearch.php?species_id=0&factor=AP-1&gene=epn1&nfactor=n&ninfo=n&ngene=n&B2=Search. The EpiTect Champion ChIP Transcription Factor Portal from SAbioscience's DECODE database, JAPSER and Ensemble programs were utilized to identify candidate downstream transcriptional machineries involved in epsin expression. The candidate AP-1 regulatory sequences on mouse epsin 1 promoter were selected by searching the highly-conserved AP-1 regulatory sequences on human epsin 1 promoter.

Luciferase Assay

The truncated fragments of epsin 1 promoter, which include potential AP-1 binding sequences, were inserted into the luciferase reporter vector pGL4.23 [luc2/minP] (Promega) in the sense orientation. Primary LECs isolated from mice with or without STZ-induced diabetes were incubated in 6-well plates

for 24 h. When the confluency reached 70%, cells were transfected with 1µg of reporter plasmid and 1µg of effector plasmids using Lipofectamine® LTX Plus DNA transfection reagents according to the manufacturer's protocol. Cells were harvested after 48 h transfection, and cell extracts were subjected to a luciferase assay using the Dual Luciferase Reporter Assay System (Promega), in which Renilla luciferase plasmids were co-transfected as controls to standardize the transcription efficiency. The mutations were created in the AP-1 binding sites within the epsins promoter-driven luciferase reporter plasmids using the Quick Change Site-Directed Mutagenesis Kit according to the maufacturer's. To check luciferase activities by using AP-1 blocking peptide, 20 µM AP-1 blocking peptides were added into the passive lysis buffer (PLB) of the LECs and incubated at 4^0C for 4 h, then measured the luciferase activities.

Chromatin immunoprecipitation (ChIP) assay

ChIP assays were performed using the ChIP Assay Kit (QIAGEN) according to the manufacturer's protocol. Briefly, LECs from mice with or without STZ-induced diabetes were incubated in 10-cm-diameter dishes for 24 h. Cells were cross-linked by treating with 1% formaldehyde for 10 min at 37°C. After washing with 1X PBS, cells were pelleted and resuspended in lysis buffer. The lysates were then subjected to sonication to shear the DNA length between 500 bp to 1000 bp. Precleared samples by incubation with DNA-protein A agarose slurry for 50 min at 4^0C. The supernatant was incubated with anti-AP-1, and anti-IgG and anti-GAPDH antibodies at 4^0C for o/n. Immunocomplexes were collected with DNA-protein A agarose slurry and eluted after extensive washing. The cross-linkage was reversed by heating at 65^0C, followed by treated with proteinase K at 45^0C for 30 min and then at 95^0C for 10 min. DNA was recovered by DNA purification spin column and used as a template for PCR to amply the region including the AP-1 binding site. The primer pairs for AP-1 binding site of human epsin 1 promoter: sense, 5'-GATGATGCTAGCCATGATGGATTTCTTCAACGC-3'; anti-sense, 5'-CTACTACTCGAGTCCTGCCTGACACAGATGTGC-3'. The primer pairs for AP-1 binding site of mouse epsin 1 promoter: sense, 5'-CTTAACTGTCCAGCATCATTATG-3'; antisense, 5'-CCCCAGAGATGAAGTGACAATAC-3'.

RNA interference for Knock down c-Src

LECs isolated from mice with or without STZ-induced diabetes were incubated 6-well dish plates for 24 h. When the confluency reached 70%, cells were starved and incubated at 37^0C for 8 h or o/n. The c-Src siRNA was transfected around 0.3 µM by Lipofectamine® RNAiMAX™ into 6-well plates. Cells were incubated at 37^0C for 6~8 h, and then added half a volume of complete EC medium. Cells were incubated around 12 h, and then changed to the complete EC medium, and continually incubated another one day. The siRNA targeting sequence on mouse Src is CCCAGACTTGTTGTACATATT. The designed siRNA sequences for mouse c-Src were purchased from Life Technologies: sense: 5'-CCCAGACUUGUUGUACAUAUU-3'; antisense: 5'-AAUAUGUACAACAAGUCUGGG-3'.

Preparation of LECs from diabetic patients and non-diabetic persons

Eleven patients with type 2 diabetes mellitus (stage III) and eight non-diabetic persons were enrolled. Patients were diagnosed in the Second Xiangya Hospital, Central South University, China, according to the World Health Organization's diagnostic criteria for type 2 diabetes. Vessels were surgically removed and collected when patients underwent arteriovenous fistula surgery. Specimens were stored in liquid nitrogen. All procedures were carried out in accordance with the approved guidelines, and the research has been approved from the human research ethics committee of the Second Xiagya Hospital, Central South University. Informed consent was obtained from all the participants.

Mouse corneal micropocket lymphangiogenesis assay

The corneal micropocket lymphangiogenesis assay was performed as described previously (9, 10) using implants containing VEGF-C, hydron and sucralfate. VEGF-C (C152S, RLT-R20-017; ABIN2018451 or ABIN2003025) were around 160 ng per pellet. Implants containing hydron and sucralfate alone served as negative controls. The mice were anesthetized by intraperitoneal injection of 2.5% avertin (400-500 $mg\,kg^{-1}$). The eyes were topically anesthetized with one drop of 0.5% proparacaine per eye. An incision was created using a 30^0C angle and were gently proptosed with forceps. Using a corneal blade and a stereoscope, intrastromal linear keratotomy was performed about 0.7-1.0 mm from the limbus. Using a von Graefe knife (Miltex), a pocket was extended

towards the limbus, and the volume of 0.4 mm x 0.4 mm x 0.2 mm pellet of VEGF-C was manoeuvered into the pocket. The wound was coated with a lubricant ophthalmic ointment (Rugby) to prevent infection. Mouse corneas were harvested 7 days after pellet implantation, fixed in 4% paraformaldehyde/PBS (1 h at room temperature), washed with PBS. To quantitate the extent of lymphangiogenesis, flat mounts of the dissected corneas were evaluated by fluorescence microscopy. Fluorescent images were acquired by SlideBook (Olympus), vessel areas were quantified by ImageJ. Corneas were stained with Alexa Fluor-488-anti-mouse LYVE-1 (to visualize lymphatic vessels) and Alexa Fluor 594-anti-mouse CD31 (to visualize blood vessels) in 10% donkey serum/0.3% Triton X-100/PBS overnight, 4 °C. After several washes with 0.3% Triton X-100/PBS, the corneas were flattened and mounted with VECTASHIELD mounting medium (Vector Laboratories) and evaluated by fluorescence microscopy. Fluorescent images were acquired by SlideBook (Olympus). Total lymphatic vessel growth pixels were quantified using Adobe Photoshop. Limbi in original images (below the white broken lines in Figure 1D) were removed prior to calculating total number of pixels in vessels using Adobe Photoshop's histogram tool on the LYVE-1 channel. Vessel growth pixels of mice were calculated by normalizing their ratios with WT images.

Z-stack images of corneal lymphangiogenesis

To quantitate lymphangiogenesis, corneal flat mounts of the dissected corneas were evaluated by fluorescence confocal microscope (ZEISS LSM-880, Oberkochen, Germany), and lymphatic vessels imaged at 20X and 40X magnification. At multiple sites within each sample, 0.5-µm z-axis steps were taken. Image construction and orthogonal viewing on the image stacks were performed using the Zeiss Zen Black software and image J. Maximal intensity projections representatives of the data are shown.

Preparation of corneal single-cell suspensions and flow cytometry

The corneal single-cell suspensions and lymphangiogenesis assay by flow cytometry were described previously (11). Briefly, after implanted VEGF-C (C152S, RLT-R20-017; ABIN2018451 or ABIN2003025) on Day 7, whole corneas were carefully isolated from above the limbus of mouse eyeballs, placed in ice-cold PBS and cut into small fragments using a scalpel blade. Corneal fragments were then digested in 2 mg ml^{-1} collagenase IV (Invitrogen)/PBS for 30–45 min at 37 °C

with gentle shaking. The resulting cell suspensions were then passed through a 70 μm cell strainer into 1X HBSS/25 mM HEPES/2% newborn bovine calf serum (staining medium). Cells were subsequently washed twice with FACS staining medium and then stained according to standard flow cytometry protocols with anti-mouse LVYE-1 biotin (1:20, Thermo Fisher Scientific), followed by streptavidin-Alexa-594 (1:200, eBiosciences). Data acquisition was performed using a Cyan flow cytometer (Dako) and analysed using FlowJo software (Tree Star).

Matrigel plug assay

Mice were injected subcutaneously with 0.5 ml Matrigel (356230; BD Bioscience) containing PBS, 2μg VEGF-C (2179-VC; R&D system). Eight days after implantation, the Matrigels were harvested, and cryosections (10 μm) were prepared for immunohistochemistry. Cryopreserved in Tissue-Tek OCT (Sakura). Cryosections were processed for immunofluorescence staining using anti-LYVE-1 and VEGFR3 antibodies. Digital images of staining were obtained using confocal microscopy. Quantification analysis for LYVE-1 and VEGFR3 in Matrigels were performed using Scion Image software. WT (n=5), LEC-iDKO (n=5), WT/STZ/HFD (n=5), and LEC-iDKO/STZ/HFD (n=5) mice were performed Matrigel assay.

Visualization of lymphatic vessel transport by Intravital Multiphoton Microscopy

To examine mouse tail lymphatic vessel transport, FITC-dextran (2000-kD, 300 μl/Kg body weight) was injected to the tail (approximately 10 mm proximal to the body) of WT (n=5), LEC-iDKO (n=5), WT/STZ/HFD (n=5) and LEC-iDKO/STZ/HFD (n=5) mice at postoperative Day 30. Before injection, mice were anesthetized with 2% isoflurane and placed on a heating pad. Animals were positioned under the intravital multiphoton microscopy system such that the field of view captured the tail. Migration of fluorescence, towards the dismal end of the tail, was followed every 5 minutes for 15 minutes after injection. Images were collected at 0, 5, 10 and 15 minutes with a 1.25X lens, NA 0.04 (Olympus America, Center Valley, PA), on an Olympus FV1200-MPE multiphoton imaging system coupled to a Ti:sapphire MaiTai DeepSee laser (Newport/Spectra Physics, Santa Clara, CA). Excitation light of 800 nm was used and fluorescence emission was detected via a 500-550 nm bandpass filter. Images were reconstructed from Z-series scans, covering a depth of 600 μm, using Olympus Fluoview FV10-ASW, v

4, software (Olympus America). Images shown in the figures represent an area of approximately 16 mm x 9 mm resulted from stitching together two or three images from adjacent areas. A trans-illumination channel (non-fluorescence) was also collected simultaneously and merged with the fluorescence channel, giving a lighted background to delineate the outline of the tail. The locations of the injection sites, as well as the wounded and neighboring areas were shown with improved clarity relative to one another.

Near-infrared (NIR) imaging of lymphatic transport in vivo

NIR imaging was used to examine if functional differences exist in lymphatic transport between WT and LEC-iDKO adult mice upon deletion of epsin by administration of 4-hydroxytamaxofin. Briefly, 10 μL of LI-COR IRDye 800CW (LI-COR Biosciences, Nebraska, USA) covalently labeled to 40 KDa PEG through an NHS-esther linkage as described previsouly (12) was injected intradermally into the tip of the tail for fluorescence imaging. An injection volume of 10 μL was chosen based upon past success in rodent models, so as to not overload the lymphatics with unnecessary fluid volume while at the same time providing enough tracer for sufficient detection (13). The injection was given at an entry angle of approximately 10 degrees to an approximate depth of 1 mm to specifically target the lymphatic vasculature intradermally. Care was taken to position the injection as close to the midline of the tail as possible to avoid favoring one collecting vessel over the other. Images were taken with a customized imaging system consisting of a Shutter Instruments Lambda LS Xenon arc lamp, an Olympus MVX-ZB10 microscope, a 769 nm bandpass excitation filter (49 nm full-width half maximum, FWHM), an 832 nm bandpass emission filter (45 nm FWHM), and an 801.5 nm longpass dichroic mirror. Images were acquired with a Photometrics Ecolve Delta 512 EM-CCD. Field of view was centered on the mouse's tail 7cm caudal from the injection site. This location ensured that only the downstream collecting lymphatics would be visualized. The small volume of fluid injection and the use of NIR to enhance tissue penetration ensures that only fluorescence in the deeper collecting lymphatics is visible downstream of the injection site. The animals were imaged continuously from the time of injection until 20 minutes post-injection with a 50ms exposure time and a frame rate of 10 fps. Analysis of NIR functional metrics was performed during the steady-state period from 5-20 minutes after injection, as defined previously (14). NIR function was evaluated by quantifying the temporal fluctuation in fluorescence observed in a specified ROI downstream of the injection site.

Mouse tail edema model

To establish tail edema, circumferential incisions were made through the tail dermis 1 cm away from the tail base of 11-13 week-old WT (n=8), LEC-iDKO (n=8), WT/STZ/HFD (n=8), and LEC-iDKO/STZ/HFD (n=8) mice as previously described (6). To create an inducible lymphatic endothelial cell-specific epsin deletion driven by our *Prox1-Cre-ER^{T2}* mouse model, we administered 4-hydroxytamoxifen into 8-10 week-old adult mice. These mice were injected with 4-hydroxytamoxifen (0.3mg/30gram body weight) every other day, for a total of 5 injections continuously. Finally, at week 10-12, WT and LEC-iDKO mice were STZ treated for 5 days to induce hyperglycemia, and then fed with 8-12 weeks of high fat diet to maintain hyperglycemia mimicking the conditions of Type 2 diabetes. The incision was subsequently scratched with a razor blade to generate a 3-4 mm gap to damage the lymphatic vessels in WT, LEC-iDKO, WT/STZ/HFD, and LEC-iDKO/STZ/HFD mice. Tail volumes were analyzed using following volume displacement as previously described (6). Quantification of tail volume distal to the incision of postoperative tail edema of mice at postoperative Days 1, 7, 10, 14, 18, 21, 24, and 28 respectively.

$V_1 = \pi$ (3.14) X square of the radius of the measure site X h (the distance from the measure site to the tip of the tail) / 3;

V = Scraped tail area average volume = $(V_1 + V_2 + V_3 + V_4 + V_5 + V_6 + V_7 + V_8) / 8$;

Day n swollen percentage = $(V_{Day\,n}/V_{Day\,0} - 1)$ X 100%

On day 30, the circumferential incisions were biopsied to include the margin of normal surrounding skin, fixed in 4% paraformaldehyde overnight, and then cryopreserved in Tissue-Tek OCT (Sakura). Cryosections were processed for immunofluorescence staining using anti-LYVE-1, anti-VEGFR3, anti-VEGF-C antibodies.

Glucose tolerance test (GTT)

Mice were fasted overnight for about 16 hours. The weight of each mouse determined the calculated glucose dose at a ratio of 2.5 g/kg body weight. Injection volume into the peritoneal of mouse = BW(g)X10 ul of 250mg/ml glucose solution. Tail snipping was used to collect blood samples. Blood glucose was determined by glucometer in tail vein blood. The blood glucose of each mouse was

measured to determine the value for the 0 time point. Blood glucose is measured at 15, 30, 60, 90, and 120 minutes after the glucose injection.

Insulin tolerance test (ITT)

Mice are fasted for six hours. The weight of each mouse determined the calculated insulin dose at a ratio of 0.75 U/kg body weight. Insulin was prepared at 0.1 U/ml in advance (16.6 µl of 10 mg/ml insulin in 40 ml PBS). Injection volume into the peritoneal of mouse = BW(g) X 7.5 µl of 0.1U/ml insulin solution. Tail snipping is used to get blood. Blood glucose level were determined by glucometer in blood from tail vein. Measured blood glucose of each mouse to get the value for 0 time point. Blood glucose was measured at 15, 30, 60, 90, and 120 minutes after the insulin injection.

Primary mouse lymphatic endothelial cell isolation and culture

Primary mouse LECs were isolated from the skins of 8-10 week-old WT, LEC-iDKO, WT/STZ/HFD, and LEC-iDKO/STZ/HFD mice as previously described (15, 16). Breifly, finely minced skin or mesentery tissue was digested with enzyme solution [collagenase (2 mg/ml), dispase (5 mg/ml); Roche] at 37°C for 1 hour, and cells were cultured in complete endothelial cell medium (Invitrogen). Then, rat anti-mouse LYVE-1 monoclonal antibody (ALY7, eBioscience ^{TM}) was incubated with primary cells at room temperature around 1 h. After washing with MACS buffer, LECs were further purified using goat anti-rat IgG Microbeads according to manufacturer's instructions, and eluted cells reapplied to a fresh MACS MS column (16). Isolated primary LECs were immediately seeded into the complete endothelial cell medium (Invitrogen) in pre-coated 0.1% gelatin cell culture plates. The identity of LECs was confirmed with LYVE-1 immunofluorescence staining and VEGFR3 flow cytometric analysis. LEC purity (>90%) was measured by the expression of LYVE-1 and VEGFR3. Deletions of epsins 1 and 2 were confirmed by RT-qPCR and Western blotting (4).
LECs cultured under high-glucose were grown in the presence of 22 mM glucose for a minimum of 5 days prior to experimentation. For the LECs treated with H_2O_2 and/or NAC (N-acetyl-L-cysteine), LECs were cultured in 5 mM glucose, treated without or with 5 mM NAC for 30 min followed by 500 µM H_2O_2 for 15 min. Treated LECs were lysed and analyzed by Western blotting as indicated.

Whole-mount of mesenteric lymphatic vessels and imaging

Mouse mesenteric tissues were removed post mortem and pinned out into loops in PBS on a Sylgard-coated dish as indicated by previous studies (4). These loops were fixed with 2 % paraformaldehyde solution at room temperature and permeabilizing in 0.01% Triton X-100. The mesenteric arcades were cut from the intestinal wall, and at least two mesenteric bundles were incubated in block solution (5% donkey serum, 0.01% Triton X-100) for 2 h at room temperature. The tissue arcades were then incubated with primary antibodies against Prox1 (1:100) and integrin α 9 (1:100) overnight. Donkey anti-rabbit/anti-goat antibodies were incubated for 2 h. Tissues were mounted with antifade mounting reagent. Images of lymphatics were taken using confocal microscope (ZEISS LSM-880, Oberkochen, Germany) at 488 nm or 594 nm, and were collected with 20X and 40X magnification with lymphatic vessels centered in the field of view (FOV) respectively. At multiple sites within each sample, 0.5-μm z-axis steps were taken. The images were focused around mesenteric collecting lymphatics and valve regions. Lymphatic vessels were determined by their morphology with the presence of bulbar valve regions, and Prox1 positive cells were used as a marker to verify lymphatic endothelium. Image construction and orthogonal viewing on the image stacks were performed using the Zeiss Zen Black software and image J. The negative controls for all experiments were produced and analyzed via the same instrumental and image-processing produces. Maximal intensity projection representatives of the data are shown. NIH Image J edge finder and plug-in colocalization were used to quantify valve leaflet depth, perimeter, and Prox1+ cells as described in the previous study (4, 17).

Immunostaining

For whole-mount tissue staining, mesentery or ears were dissected, fixed in 4% PFA and blocked in phosphate buffered saline (PBS) solution containing 5% donkey serum and 0.3% Triton X-100; For staining of tissue sections, lymph nodes or mouse tails were processed and embedded in paraffin. Five micron sections were cut and deparaffinized using xylene and descending alcohol series. H & E staining was accomplished using standard procedures. Oil red O staining was accomplished as previously described in the manufacturer's protocol (NovaUltra Special Stain Kit). For immunofluorescent staining, antigen retrieval was performed using 1X proteinase K (0.01 mg/mL) solution. Samples were blocked in PBS solution containing 5% donkey serum and 0.3% Triton X-100 then incubated with the specified

primary antibodies overnight at 4°C, followed by incubation with the respective secondary antibodies conjugated to fluorescent labels (Alexa Flour) for 1 h at room temperature. Samples were washed, coverslips mounted using Vectashield permamount mounting medium and photomicrographs obtained using an Olympus Plan Apochromat objective and Hamamatsu Orca-R2 monochrome digital camera.

Western blotting

Western blotting analyses were performed according to standard procedures using specified antibodies. All Western blotting quantifications were performed with National Institutes of Health (NIH) ImageJ software.

Cell surface biotinylation assay

Primary LECs were cultured in 5 mM or 22 mM glucose for a minimum of 5 days. LECs were starved overnight prior to being stimulated with 100 ng/mL VEGF-C (2179-VC; R&D system) for 10 min. After stimulation, LECs were incubated with 1 mM EZ-Link Sulfo-NHS-LC-Biotin on ice for 30 min then washed with 50 mM glycine. LECs were lysed using RIPA buffer and processed for streptavidin bead pull down. Cell surface biotinylated VEGFR3 was analyzed by Western Blotting using anti-VEGFR3 antibodies and quantified by NIH ImageJ software.

Cell surface proteolysis assay

LECs were serum starved overnight and then treated with 0.25% trypsin plus 0.02% EDTA in PBS for 45 s to cleave cell surface proteins. The reaction was quenched with complete medium. Cells were treated without or with 500 µM H_2O_2 or 100 ng/mL VEGF-C (2179-VC; R&D system) for 10 min. Cells were lysed and analyzed by Western blotting for VEGFR3 phosphorylation, VE-cadherin. Anti-VE-cadherin antibody recognizes the extracellular domain of VE-cadherin, thus acting as a positive control for trypsin digest. Prior to trypsin digest, the anti-VE-cadherin antibody detects full-length VE-cadherin; however, after trypsin digest, the anti-VE-cadherin antibody recognizes the 21 kDa cytoplasmic domain of Ve-cadherin which, due to SDS-PAGE limitations, is no longer detectable. Therefore, loss of full-length VE-cadherin detection acts as an additional positive control for the trypsin digest.

Antibody feeding assay

LEC cells of WT, LEC-iDKO, WT/STZ/HFD and LEC-iDKO/STZ/HFD were serum-starved overnight and stimulated with 100 ng/mL VEGF-C (2179-VC; R&D system) for 15 min. Cells were fixed by 4% PFA, and then incubated with rat anti-VEGFR3 extracellular domain antibody at 4^0C for 1 h. Cells were washed with 1X PBS, and incubated with secondary goat anti-rat antibody conjugated with Alexa-488 at RT for 1 h. After staining with 1 µg/mL DAPI at RT for 15 min, the total VEGFR3 on cell surfaces was detected by confocal microscopy. quantifications were performed with National Institutes of Health (NIH) ImageJ software.

In vitro LEC proliferation assays

Primary LECs were cultured on gelatin-coated coverslips until they reached 50% confluent. Cells were serum starved overnight and stimulated with/without 100 ng/mL VEGF-C for 24 h. Ki67 and Prox1 incorporation were analyzed as previously described (3).

In vitro wound healing and tube formation assays

Mouse LECs were cultured and subjected to scratch "wound injury" assay or matrigel tube formation assay as described previously (3).

Golgi apparatus isolation

Golgi apparatus was isolated from LECs using Golgi isolation kit (Sigma) according to manufacturer's instructions. Cell lysates were centrifuged at 120,000Xg for 3 hours in a discontinuous gradient of different molar sucrose concentration solution. Golgi enriched fractions was withdrawn from 1.1M/0.25M sucrose interphase. Presence of Golgi fraction was confirmed by GM-130 antibody by western blotting. Enrichment of Golgi fractions were used for the following immunoprecipitation experiments.

Immunofluorescence staining

Cells were fixed with 4% formaldehyde in PBS, permeabilized, incubated with primary rabbit anti-VEGFR3, and antibodies conjugated relative dye. Cells with then thoroughly washed, covered slips mounted, and immunofluorescence images obtained using an Olympus 1X81 staining Disc Confocal Microscope with an Olympus plan Apo Chromat 60X objective and Humamatsu Orca-R2 Monochrome Digital Camera C1D600.

Fluorometric NO determination

LEC cells isolated from WT, LEC-iDKO, WT/STZ/HFD, and LEC-iDKO/STZ/HFD mice were pre-incubated with 10 μM fluorophore 4,5-diamino-fluorescein (DAF-2) for 15 min at 24°C in darkness on a rotary shaker (100 rpm) and then rinsed with fresh suspension buffer to remove excess fluorophore. A 1 ml aliquot of 100 mM HEPES pH 7.5 was added to the cells, which were then frozen in liquid nitrogen and thawed. The resulting cell homogenate was centrifuged (10 min at 16000 g, 4 °C), and fluorescence was measured in the clear supernatant using a spectrofluorometer (SPF-500™ Ratio, American Instrument Company, MD, USA) with 495 nm excitation and 515 nm emission wavelength.

Statistical Analysis

Data was presented as the mean ± SEM. GraphPad Prism 7 or SPSS (IBM) software was used to perform the statistical analysis. Data were analyzed by the two-tailed student's t test; 1-way ANOVA, 2-way ANOVA, and 3-ANOVA followed by Tukey's post hoc analysis were used for multiple comparisons where appropriate. P value < 0.05 was considered significant.

Supplemental Tables 1-3

Supplemental table 1, Mouse models.

Mouse Strains	*Epn1$^{fl/fl}$*	*Epn2$^{-/-}$*	Promoter	*Cre*	Tamoxifen injection	Sources
LEC-DKO	fl/fl	-/-	LYVE-1	*Cre*		Embryo study in (2-4)
Prox1- Cre ER^{T2}			Prox1	*ER^{T2}-Cre*		Described previously (1)
LEC-iDKO	fl/fl	-/-	Prox1	*ER^{T2}-Cre*	i.p. adult	This study
VEGFR3-eGFP knock-in mice (*Flt4*$^{eGFP/+}$)						(4, 5)
LEC-iDKO-*Flt4*$^{eGFP/+}$	fl/fl	-/-	Prox1	*ER^{T2}-Cre*		This study (4)
db/db						JAX^{TM} mice, This study

Notices:

1, The inducible conditional LEC-iDKO mice driven by *Prox1-Cre-ER^{T2}*, which differ from the constitutive LEC-DKO mice driven by *LYVE-1-Cre*, which were used extensively in the previous studies on collecting lymphatic valve developmental (4).

2, In this study, to circumvent the developmental defects in epsin mutant mice, we crossed *Epn1$^{fl/fl}$/Epn2$^{-/-}$ mice with Prox1-Cre-ER^{T2}* deleter mice, and induced epsin deletion with tamoxifen injection in mice of 6 – 8 weeks old of age, which have completed normal developmental processes. Prior to tamoxifen induced epsin deletion, these mice exhibit normal collecting lymphatics and intact lymph transport capability compared to WT mice. We used these mice to investigate whether epsin depletion limits VEGFR3 degradation and rescues diabetes triggered impairment of lymphatic function.

3, All mouse models were used in this study were confirmed by genotype and western blotting assay.

Supplemental Table 2, Identification of the transcription factor AP-1 regulatory sequences on human and mouse epsin 1 promoter.

No.	AP-1 binding sequences on human *EPN1* promoter region[1]	AP-1 binding sequences on human *EPN1* promoter conserved in mouse *Epn1* promoter	Identification of the AP-1 binding sites on mouse *Epn1* promoter region by ChIP assay
1	GCTGACCCAG	TCTGACCCAG	√
2	CTGAGTCAG	CTGAGTCAG	X
3	TGTGACTCAC	-	-
4	GGTGGCTCAC	GGTGGCTCAC	X
5	ggtggctcac	ggtggctcac	X
6	GGTGACTGTGA	-	-
7	gatgattca	-	-

Notes:

1. AP-1 binding sequences on human *EPN1* promoter region from QIGEN database:

http://www.sabiosciences.com/chipqpcrsearch.php?species_id=0&factor=AP-

1&gene=epn1&nfactor=n&ninfo=n&ngene=n&B2=Search

2. "√" : identification of the AP-1 binding sites on mouse *Epn1* promoter region by ChIP assay; "X": not identification of the binding sequence on mouse *Epn1* promoter region by ChIP assay; "-": the AP-1 binding sites on human *EPN1* promoter dose not conserved in mouse epsin 1 promoter region.

Supplemental Table 3, Identification of the transcription factor AP-1 regulatory sequences on human and mouse epsin 2 promoter.

No.	AP-1 binding sequences on human *EPN2* promoter region	AP-1 binding sequences on mouse *Epn2* promoter region	Identification by The Champion ChiP Transcription Factor Search Portal, which is based on SABiosciences' proprietary database known as **DECODE**[1-2]
1	TGTGACTCAA	GTGACTCAG	√

Notes:

1. AP-1 binding sequences on human and mouse epsin 2 promoter region from QIGEN database:

http://www.sabiosciences.com/chipqpcrsearch.php?species_id=0&factor=AP-1&gene=epn1&nfactor=n&ninfo=n&ngene=n&B2=Search;

2. **SABiosciences' Text Mining Application**: The text-mining utility, an automated data extraction system that recognizes biological entities in published papers and other public resources and then extracts the relationships between them. It relies on multiple sources of data and processes them on a large scale to support a wide variety of internal research efforts, such as identifying genes regulated by specific transcription factors. DECODE **: DEC**ipherment **O**f **D**NA **E**lements.

Supplemental References

1. Srinivasan RS, et al. Lineage tracing demonstrates the venous origin of the mammalian lymphatic vasculature. *Genes Dev.* 2007;21(19):2422-32.

2. Chen H, et al. Embryonic arrest at midgestation and disruption of Notch signaling produced by the absence of both epsin 1 and epsin 2 in mice. *Proc Natl Acad Sci U S A.* 2009;106(33):13838-43.

3. Pasula S, et al. Endothelial epsin deficiency decreases tumor growth by enhancing VEGF signaling. *J Clin Invest.* 2012;122(12):4424-38.

4. Liu X, et al. Temporal and spatial regulation of epsin abundance and VEGFR3 signaling are required for lymphatic valve formation and function. *Sci Signal.* 2014;7(347):ra97.

5. Ichise T, Yoshida N, Ichise H. H-, N- and Kras cooperatively regulate lymphatic vessel growth by modulating VEGFR3 expression in lymphatic endothelial cells in mice. *Development.* 2010;137(6):1003-13.

6. Rutkowski JM, Moya M, Johannes J, Goldman J, Swartz MA. Secondary lymphedema in the mouse tail: Lymphatic hyperplasia, VEGF-C upregulation, and the protective role of MMP-9. *Microvasc Res.* 2006;72(3):161-71.

7. Gilbert ER, Fu Z, Liu D. Development of a nongenetic mouse model of type 2 diabetes. *Exp Diabetes Res.* 2011;2011:416254.

8. King AJ. The use of animal models in diabetes research. *Br J Pharmacol.* 2012;166(3):877-94.

9. Cao R, et al. Mouse corneal lymphangiogenesis model. *Nat Protoc.* 2011;6(6):817-26.

10. Rogers MS, Birsner AE, D'Amato RJ. The mouse cornea micropocket angiogenesis assay. *Nat Protoc.* 2007;2(10):2545-50.

11. Nowell CS, et al. Chronic inflammation imposes aberrant cell fate in regenerating epithelia through mechanotransduction. *Nat Cell Biol.* 2016;18(2):168-80.

12. Proulx ST, et al. Non-invasive dynamic near-infrared imaging and quantification of vascular leakage in vivo. *Angiogenesis.* 2013;16(3):525-40.

13. Weiler M, Kassis T, Dixon JB. Sensitivity analysis of near-infrared functional lymphatic imaging. *J Biomed Opt.* 2012;17(6):066019.

14. Weiler M, Dixon JB. Differential transport function of lymphatic vessels in the rat tail model and the long-term effects of Indocyanine Green as assessed with near-infrared imaging. *Front Physiol.* 2013;4:215.

15. Kriehuber E, et al. Isolation and characterization of dermal lymphatic and blood endothelial cells reveal stable and functionally specialized cell lineages. *J Exp Med.* 2001;194(6):797-808.

16. Kazenwadel J, Secker GA, Betterman KL, Harvey NL. In vitro assays using primary embryonic mouse lymphatic endothelial cells uncover key roles for FGFR1 signalling in lymphangiogenesis. *PLoS One.* 2012;7(7):e40497.

17. Lapinski PE, et al. RASA1 regulates the function of lymphatic vessel valves in mice. *J Clin Invest.* 2017;127(7):2569-85.

Supplemental Figure 1
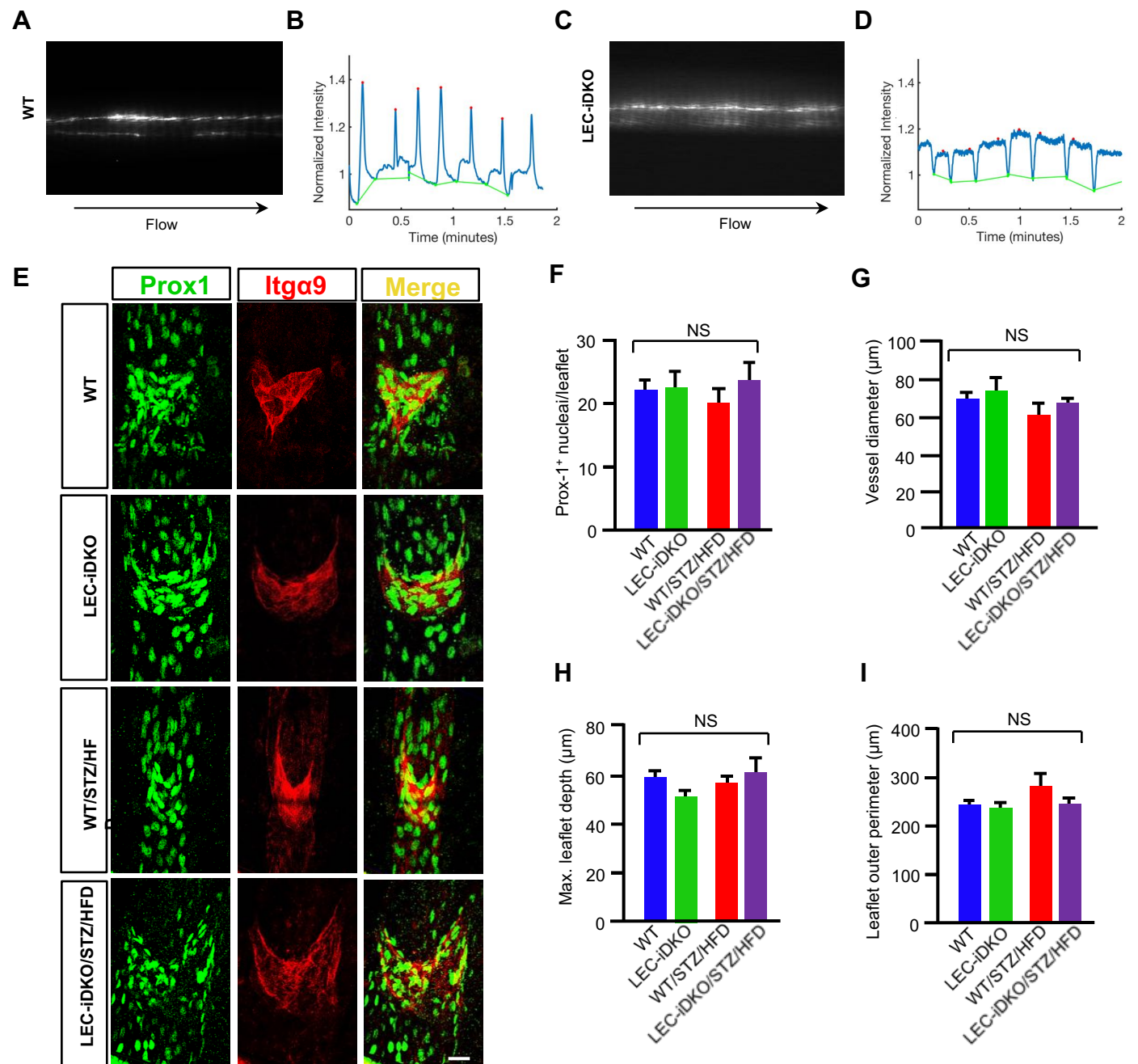
**Supplemental Figure 1. Loss of LEC epsins in adult mice has no effect on lymphatic pump function.** (**A**) Typical NIR image of collecting lymphatic transport in the tail in the WT control mice. (**B**) Representative normalized-to-baseline fluorescence intensity trace of an ROI within the tail of WT mice showing typical packet transport and frequency (n=7). (**C**) NIR image of collecting lymphatics in the tail of LEC-iDKO adult mice. (**D**) Representative normalized-to-baseline fluorescence intensity trace of an ROI within the tail of LEC-iDKO mice show typical characteristics of packet transport and frequency indistinguishable from WT controls (n=8). (**E**) Images of the whole-valve regions of lymph vessels from WT, LEC-iDKO, WT/STZ/HFD and LEC-iDKO/STZ/HFD mice. Lymph vessels were stained with integrin α-9 (red) and Prox1 (green) antibodies to highlight valve leaflets. whole-valve regions. (**F-I**) Graphs show number of Prox1$^+$ cells per leaflet (**F**), Vessel diameter (**G**), maximum leaflet depth (**H**), and leaflet outer perimeter (**I**) for different LV valve leaflets from WT, LEC-iDKO, WT/STZ/HFD, and LEC-iDKO/STZ/HFD mice (n=5). Data represent mean ± SEM, NS: not statistically significant by 2-way ANOVA. Scale bar: 20 μm.

Supplemental Figure 2

A

ITT

B

GTT

C

Lipid concentration
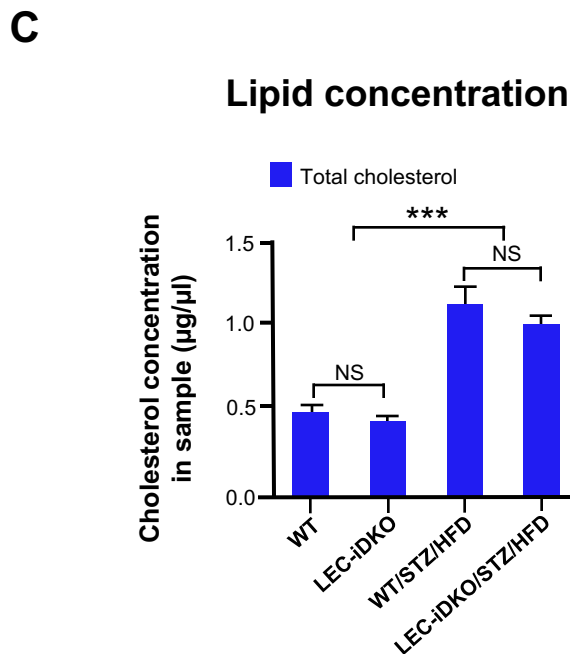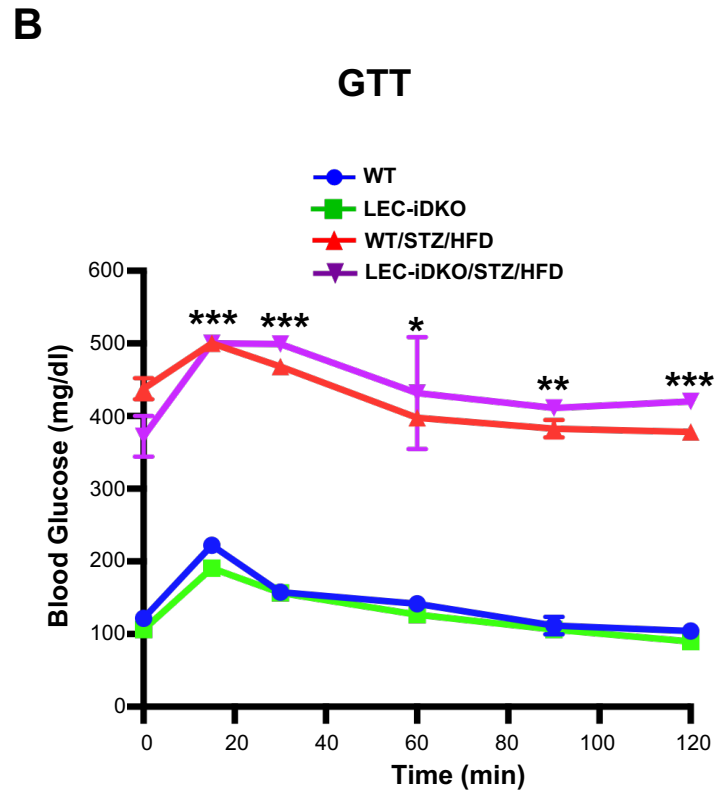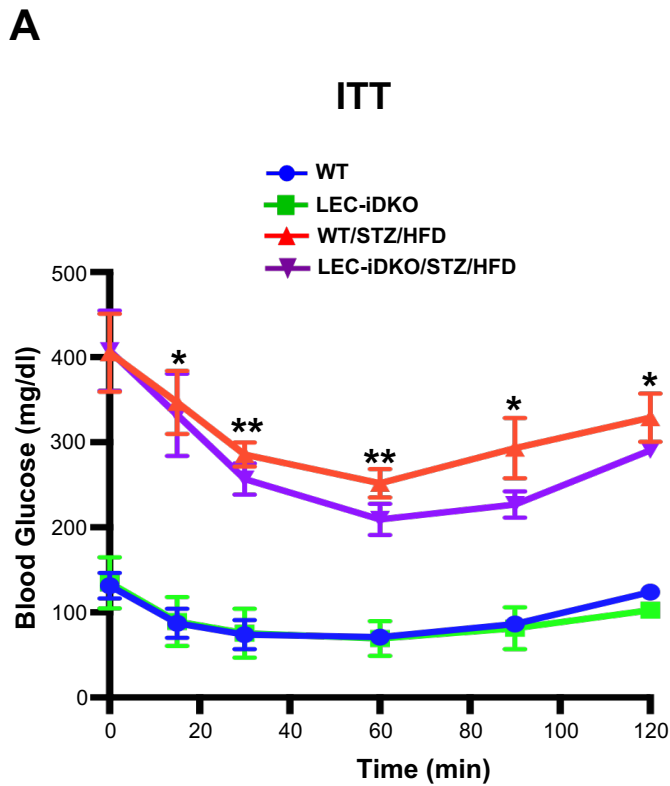
Supplemental Figure 2. STZ treatment and high fat diet induce diabetes in mice. (**A**) Insulin tolerance test (ITT), (**B**) glucose tolerance test (GTT), and (**C**) serum cholesterol levels of WT, LEC-iDKO, WT/STZ/HFD, and LEC-iDKO/STZ/HFD mice. Data represent mean ± SEM, n=8, *$P < 0.05$; **$P < 0.01$; ***$P < 0.001$, by 2-way ANOVA followed by Tukey's post hoc test. P values in A and B show significant difference of blood glucose levels between STZ/HFD diabetic groups and non-diabetic groups.

Supplemental Figure 3
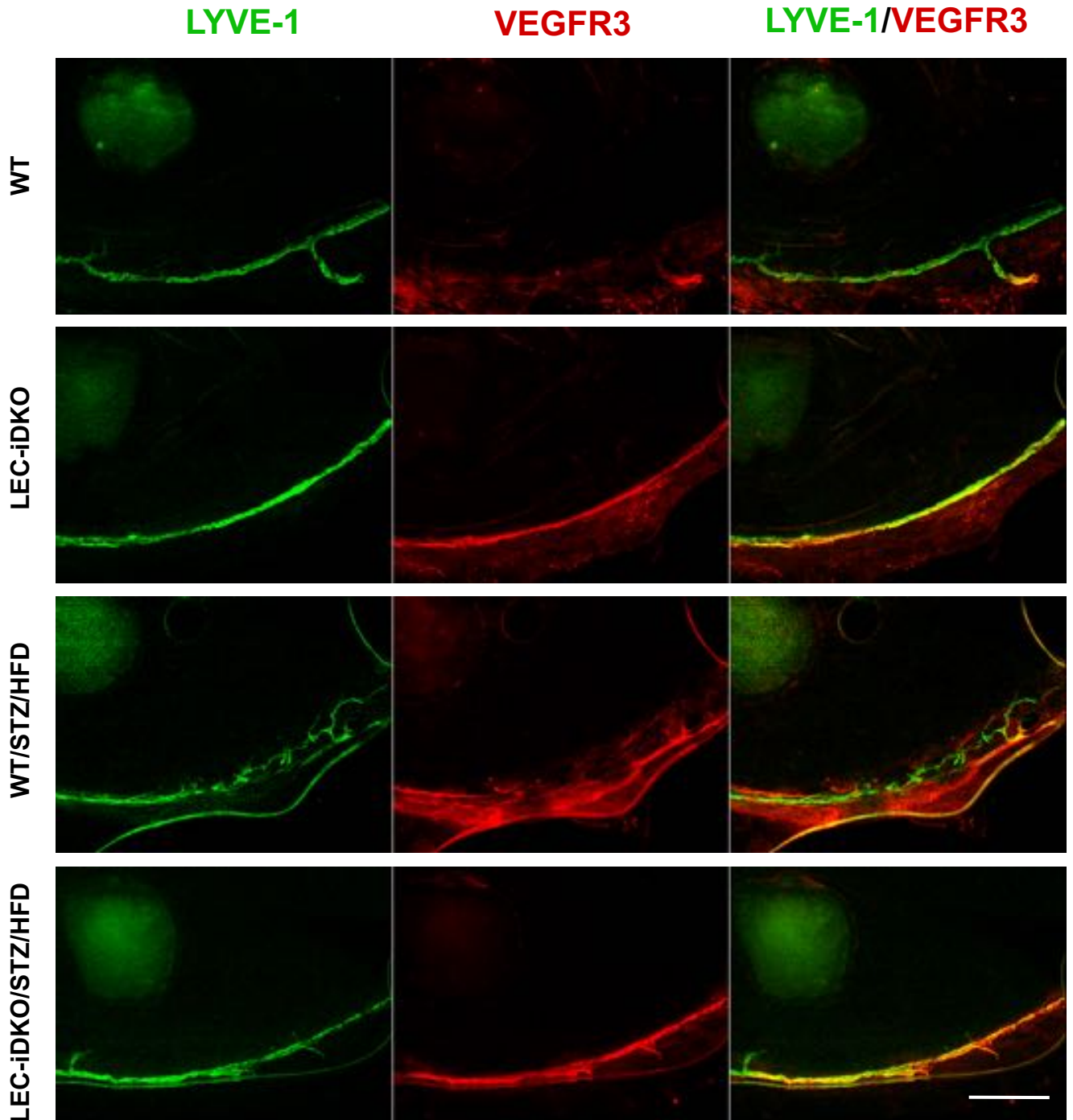
Supplemental Figure 3 (Related to Figure 1B). Whole-mount immunofluorescent staining of the control peptide-implanted corneal tissue using antibodies for LYVE-1 (green), VEGFR3 (red), at day 7 after pellet implantation. No vessel sprouting and branching were detected from WT, LEC-iDKO, WT/STZ/HFD, and LEC-iDKO/STZ/HFD mice (n=5). Scale bar: 200 μm.

Supplemental Figure 4

DAPI LYVE-1 EdU
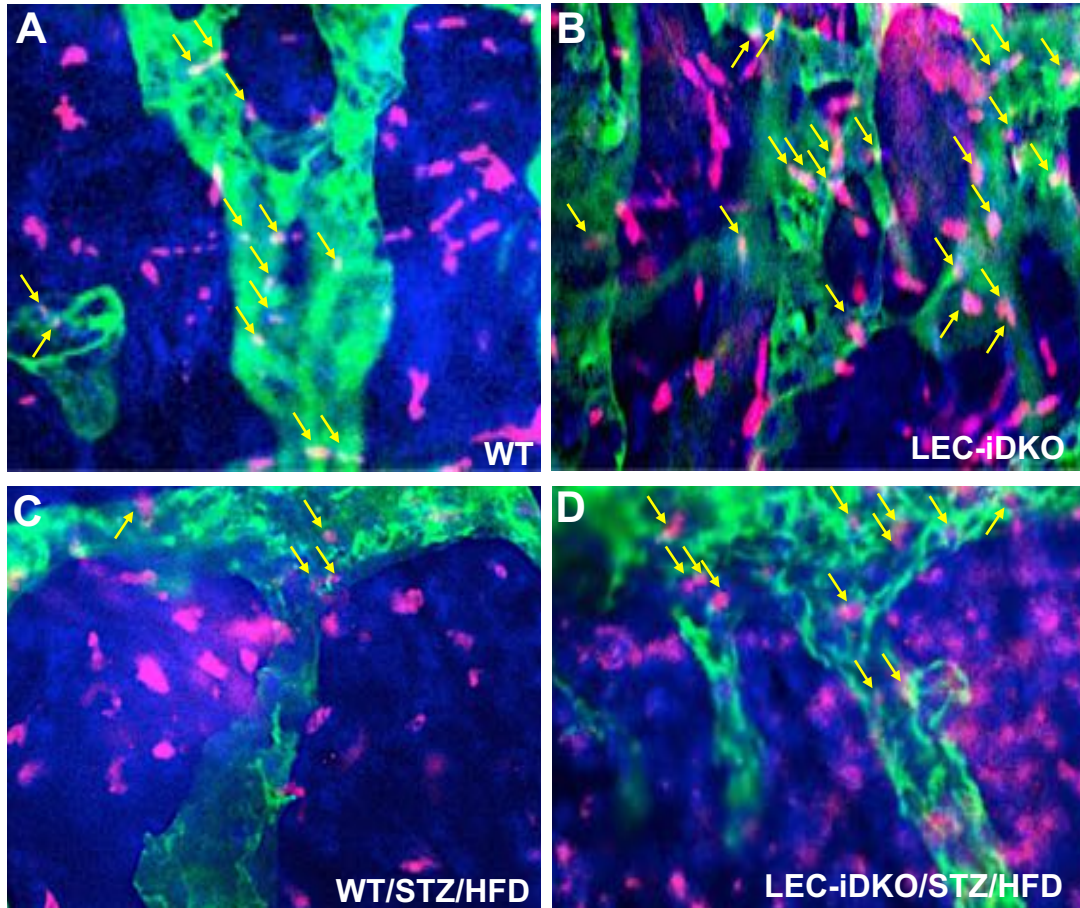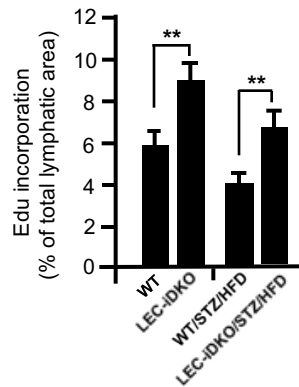
Supplemental Figure 4 (Related to Figure 1D), High magnification of confocal microscopy images show that Edu$^+$ cells are not non-LECs super imposed on LYVE-1$^+$ lymphatic structures. The neovascularization of lymphatic vessels, stained with LYVE-1 (green) and Edu (purple) in WT (**A**), LEC-iDKO (**B**), WT/STZ/HFD (**C**), and LEC-iDKO/STZ/HFD (**D**) showing significantly numerous branch points of lymphatic vessels in LEC-iDKO mice compared to that in WT mice. Quantification of Edu incorporation in lymphatic vessel in **E**. Data represent mean ± SEM, n=5, **$P < 0.01$, by 2-way ANOVA followed by Tukey's post hoc test.

Supplementary Figure 5

A WT

2.57

Counts

LYVE-1 Alexa-594

B LEC-iDKO

3.64

Counts

LYVE-1 Alexa-594

C WT/STZ/HFD

0.98

Counts

LYVE-1 Alexa-594

D LEC-iDKO/STZ/HFD

2.00

Counts

LYVE-1 Alexa-594

E Control

0.36

Counts

LYVE-1 Alexa-594

F

LYVE-1 Alexa-495 positive cells (%)

Control WT LEC-iDKO WT/STZ/HFD LEC-iDKO/STZ/HFD
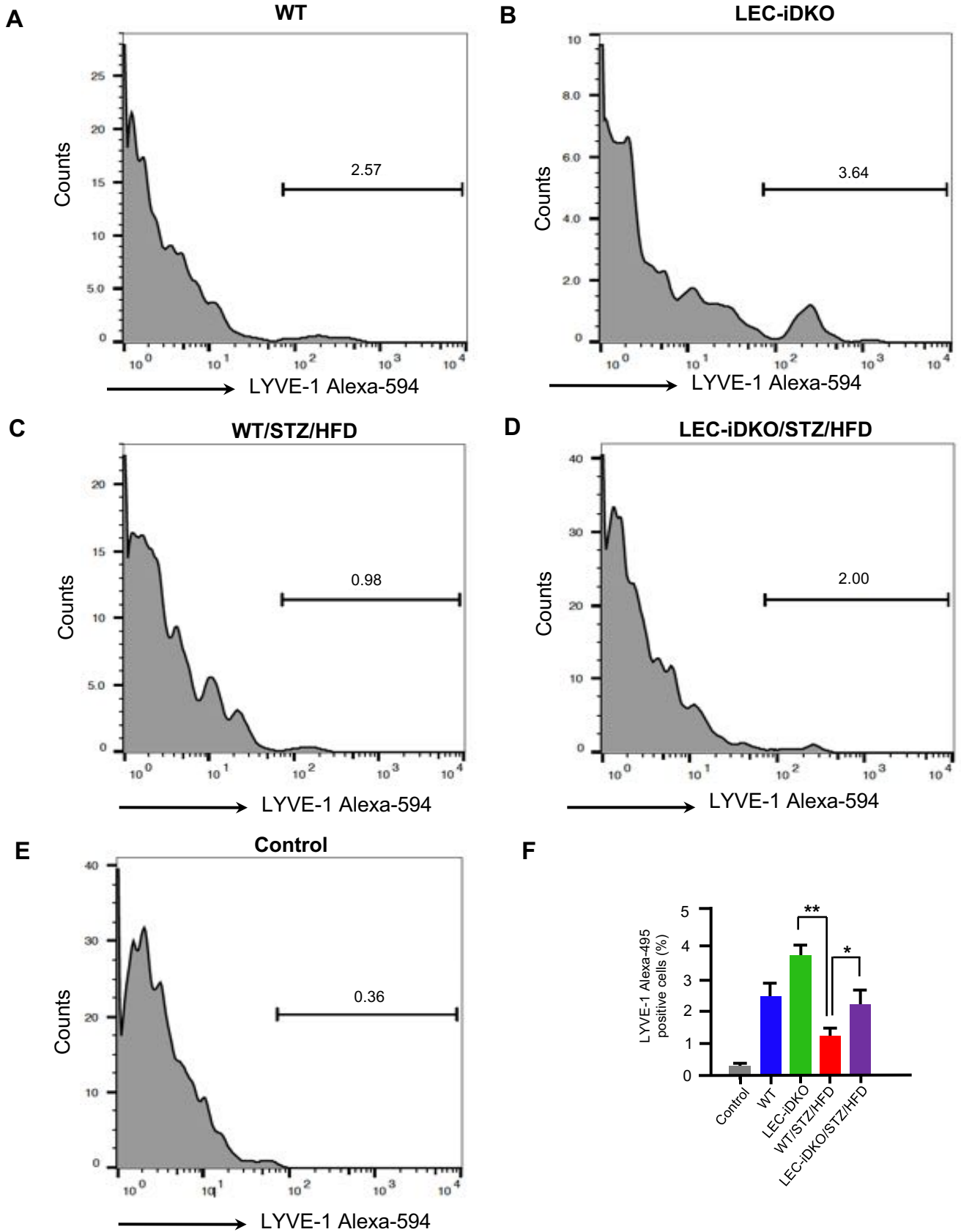
Supplemental Figure 5 (Related to Figure 1). Lymphangiogenesis in mouse corneas with VEGF-C implantation. (A-E) Flow cytometric analysis showing the proportion of total LYVE-1$^+$ cells in WT (**A**), LEC-iDKO (**B**), WT/STZ/HFD (**C**), and LEC-iDKO/STZ/HFD (**D**) mouse corneas 7 days after VEGF-C implantation. (**E**) Control: no LYVE-1$^+$ cells. (**F**) Quantifications of lymphangiogenesis in **A-E**. Data are representative of 12 individual analyses performed on cells pooled from 2 corneas of each group over three independent experiments (n=3 per group). Data represent mean ± SEM, *$P < 0.05$, by 2-way ANOVA followed by Tukey's post hoc test.

Supplemental Figure 6
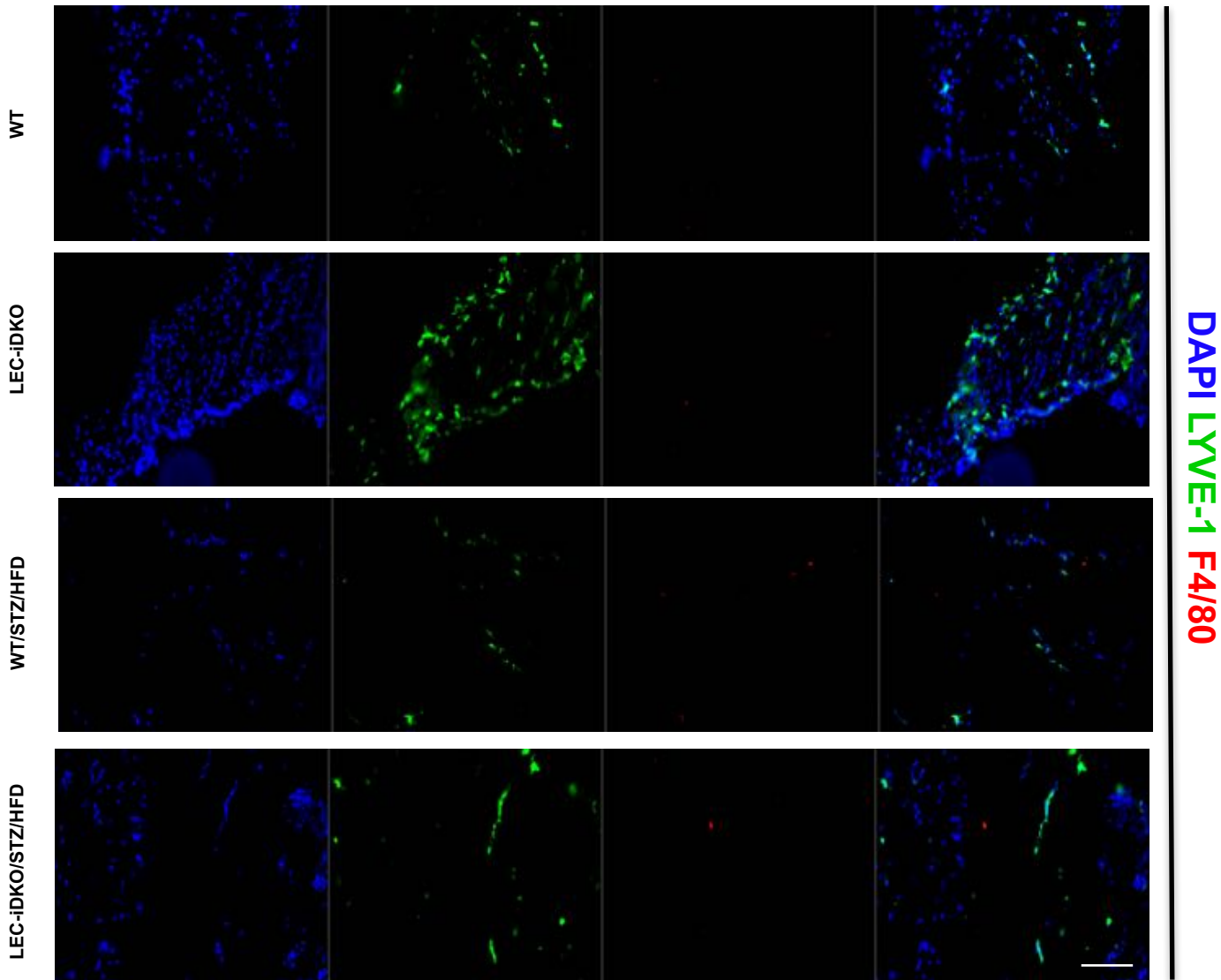
Supplemental Figure 6 (Related to Figure 1G). **Evaluation of macrophage infiltration in Matrigel plugs in WT, LEC-iDKO, WT/STZ/HFD, and LEC-iDKO/STZ/HFD mice.** Lymphangiogenesis and macrophage infiltration in Matrigel plugs containing VEGF-C were determined by using LVYE-1 (green) and F4/80 (red) antibodies. n=5. Scale bar: 50 μm.

Supplemental Figure 7
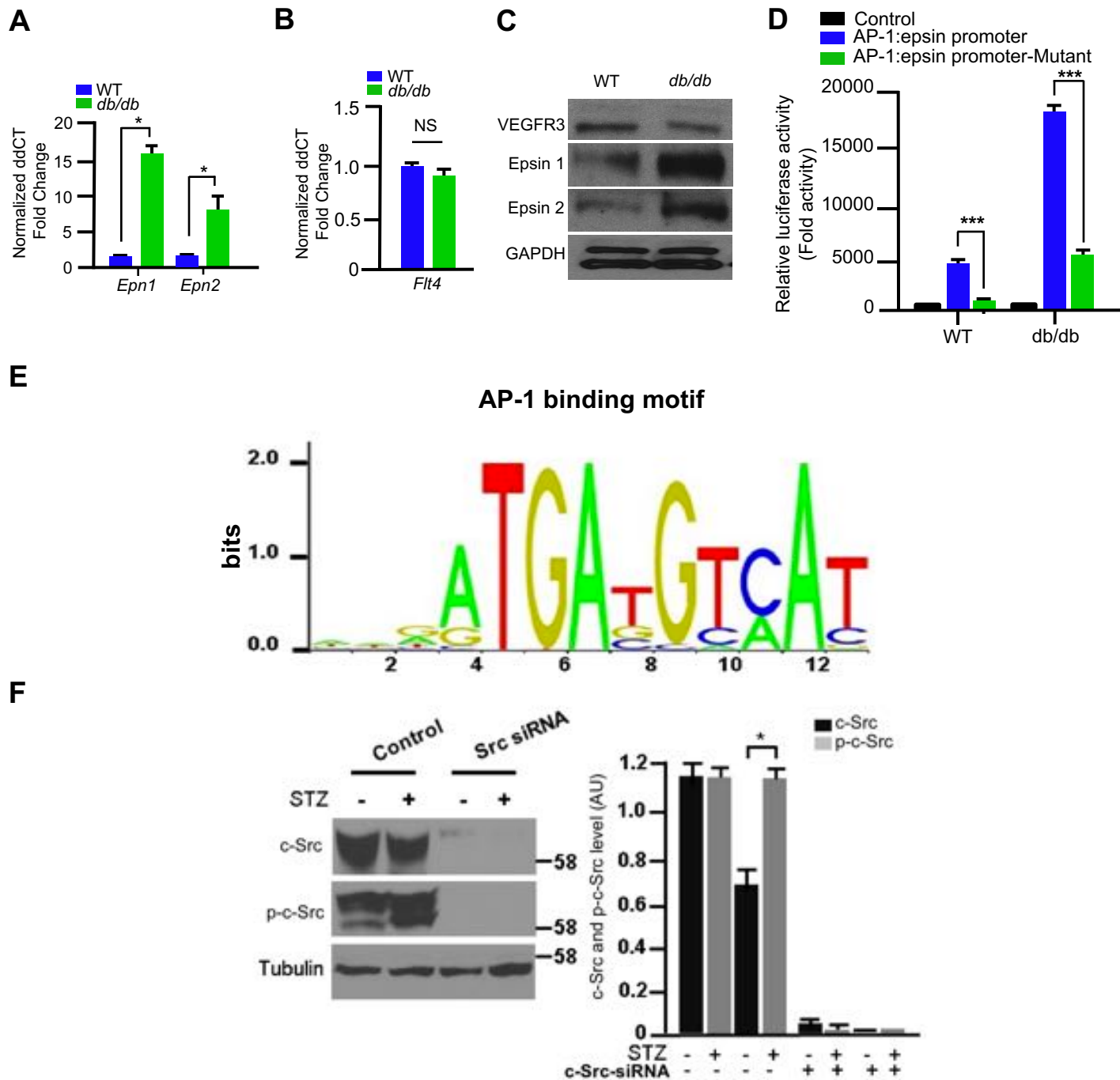
Supplemental Figure 7 (Related to Figure 2). (**A**) RT-qPCR for epsins 1 and 2 was performed in LECs of *db/db* mice and WT mice. (**B**) RT-qPCR for VEGFR3 was performed in LECs of *db/db* mice and WT mice. (**C**) Western blot analysis of epsins 1 and 2 and VEGFR3 in LECs of *db/db* mice and WT mice. (**D**) AP-1 expression vector was cotransfected with reporter plasmid pGL3-200, which harbored either WT or mutant of AP-1 binding sites, into mouse LEC cells. Blank vectors were used as control. The luciferase activities were measured and quantified. (**E**) AP-1 binding motif on epsin 1 promoter predicted by JASPAR. (**F**) c-Src knockdown in mouse LEC cells by c-Src siRNA; c-Src and Phospho-Src levels in WT and WT/STZ/HFD cells. Quantifications by using NIH ImageJ. Data represent mean ± SEM, n=5, *$P < 0.05$, 2-tailed Student's *t* test (**A** and **B**), 1-way ANOVA followed by Tukey's post hoc test (**D**), and 2-way ANOVA followed by Tukey's post hoc test (**F**).

Supplemental Figure 8

A

B
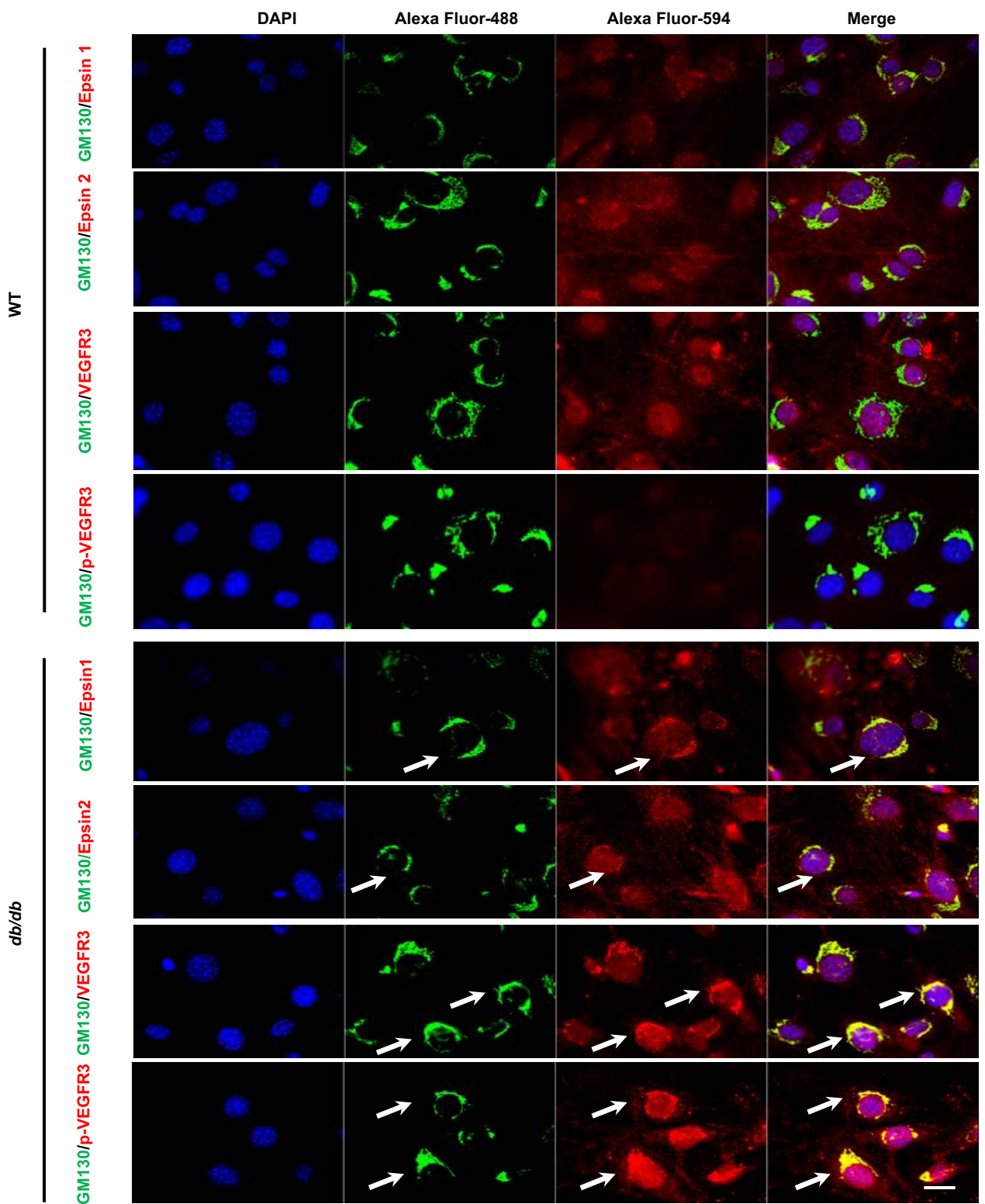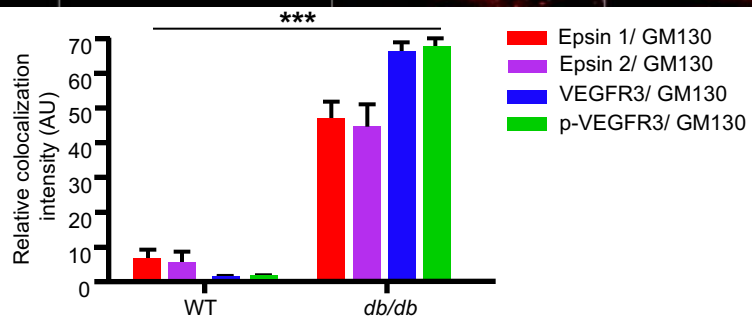
Supplemental Figure 8 (Related to Figure 6). Hyperglycemia under diabetic conditions induced phosphorylation of VEGFR3 associated with epsins in Golgi compartments in the LECs of db/db mice. (**A**) LEC cells isolated from WT and db/db mice were stained for DAPI (blue), the Golgi marker GM130 (green) and epsin 1 (red), epsin 2 (red), VEGFR3 (red), or phosphorylated VEGFR3 (red). (**B**) Quantifications of colocalization of epsins, VEGFR3 or p-VEGFR3 with Golgi marker GM130 in **A**. Arrows indicate define spots of colocalization. n=5. Quantifications by using NIH ImageJ; AU, Arbitrary Units. Data represent mean ± SEM. ***P < 0.001, by 2-tailed Student's t test. Scale bar: 20 μm.

Supplemental Figure 9

A

B
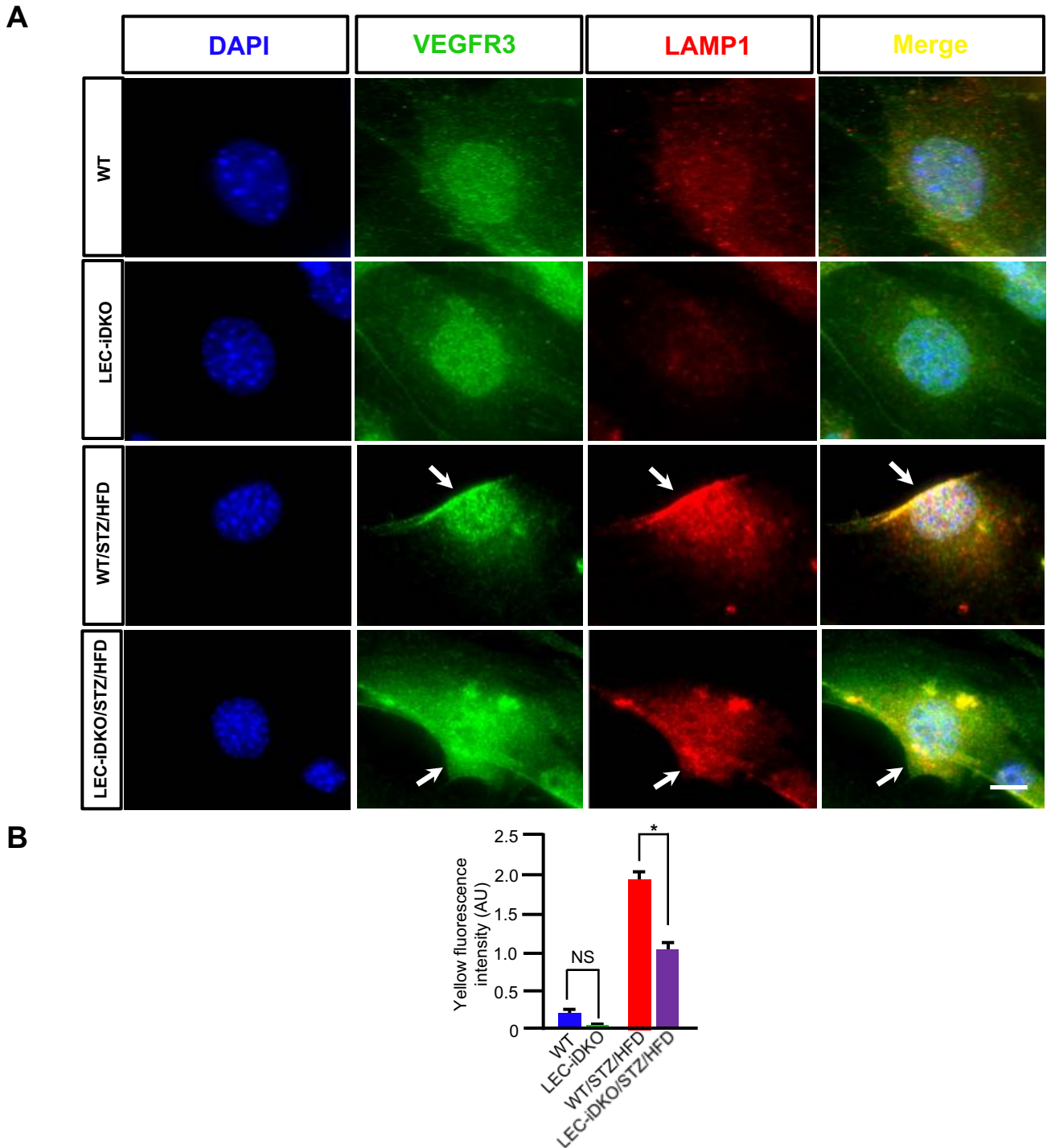
Supplemental Figure 9. Colocalization of VEGFR3 and lysosome marker LAMP1. (A) LEC cells isolated from WT, LEC-iDKO, WT/STZ/HFD, and LEC-iDKO/STZ/HFD mice and stained with antibodies for VEGFR3 (green), lysosome marker LAMP1 (red), and DAPI (blue) for Nuclei. **(B)** Quantifications of colocalization of VEGFR3 with lysosome marker LAMP1. Arrows indicate define spots of colocalization. Quantifications by using NIH ImageJ, n=5. AU, Arbitrary Units. Data represent mean ± SEM. *$P < 0.05$, by 2-way ANOVA followed by Tukey's post hoc test. NS: not statistically significant. Scale bar in **(A)**: 20 μm.

Supplemental Figure 10

A
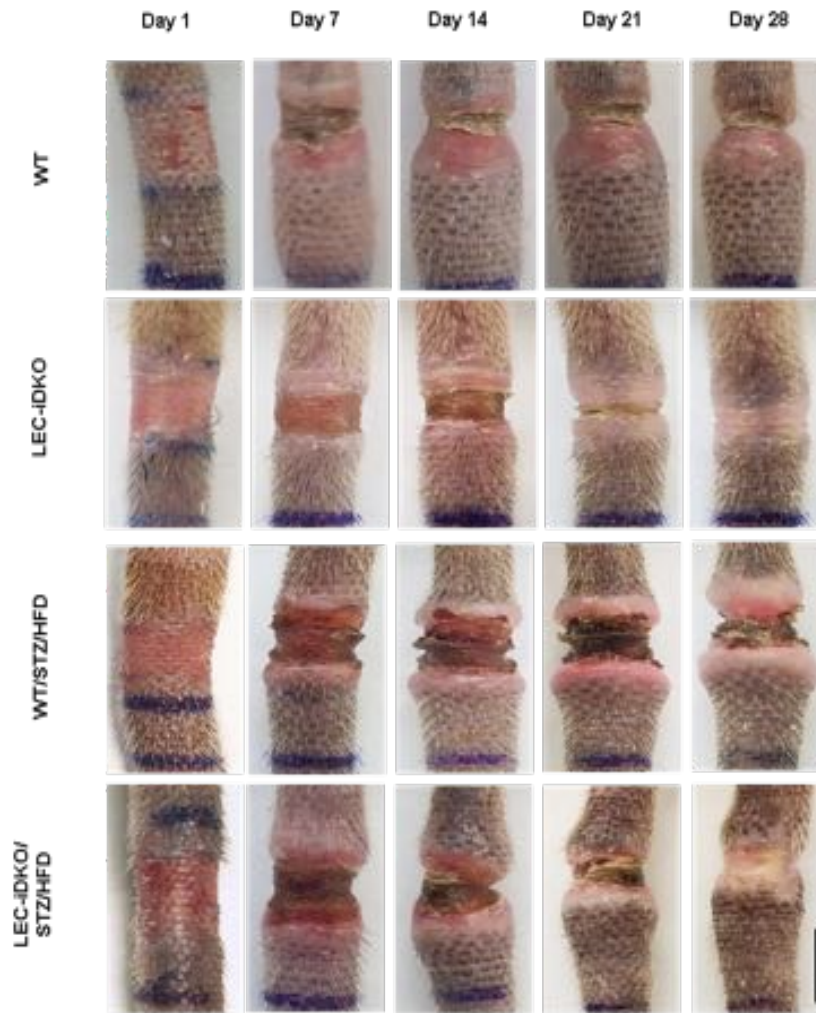
B
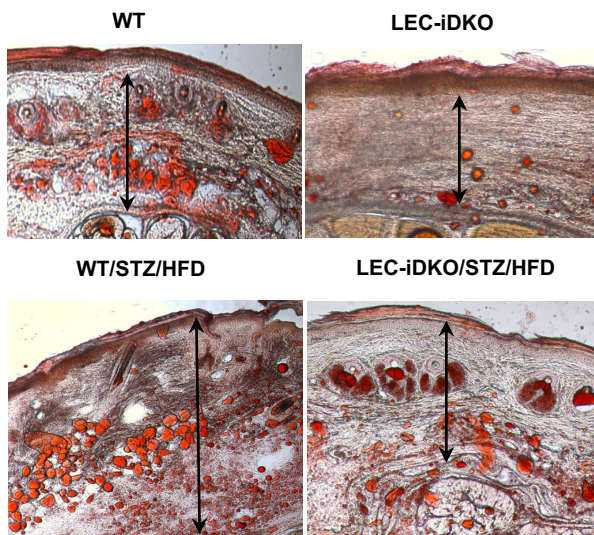
C
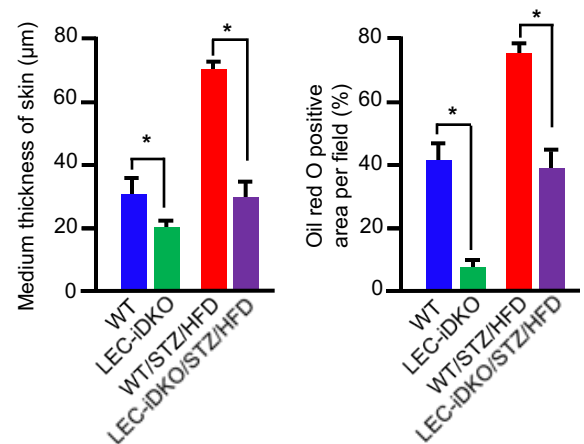
Supplemental Figure 10 (Related to Figure 7B). Mouse tail edema assay. (**A**) Representative images of postoperative tail edema of WT (n=8), LEC-iDKO (n=8), WT/STZ/HFD (n=8), LEC-iDKO/STZ/HFD (n=8) mice at postoperative Days 1, 7, 14, 21, and 28 respectively. (**B**) Representative images of Oil red O stained sections of WT (n=5), LEC-iDKO (n=5), WT/STZ/HFD (n=5), LEC-iDKO/STZ/HFD (n=5) mice at postoperative Day 30. (**C**) Quantification of medium thickness of mouse skin (indicated by double arrows and Oil red O accumulation in **B**. Quantifications by using NIH ImageJ. Data represent mean ± SEM. *$P <$ 0.05, by 2-way ANOVA followed by Tukey's post hoc test. Scar bars: 8 mm in (**A**), 100 μm in (**B**).

Supplemental Figure 11
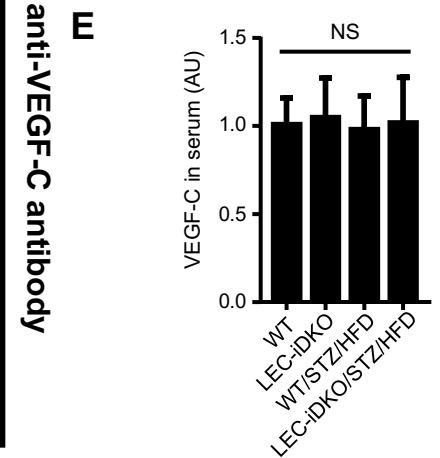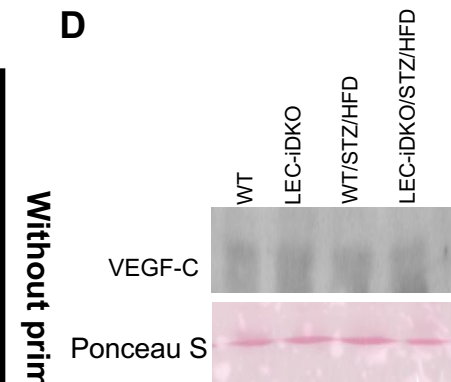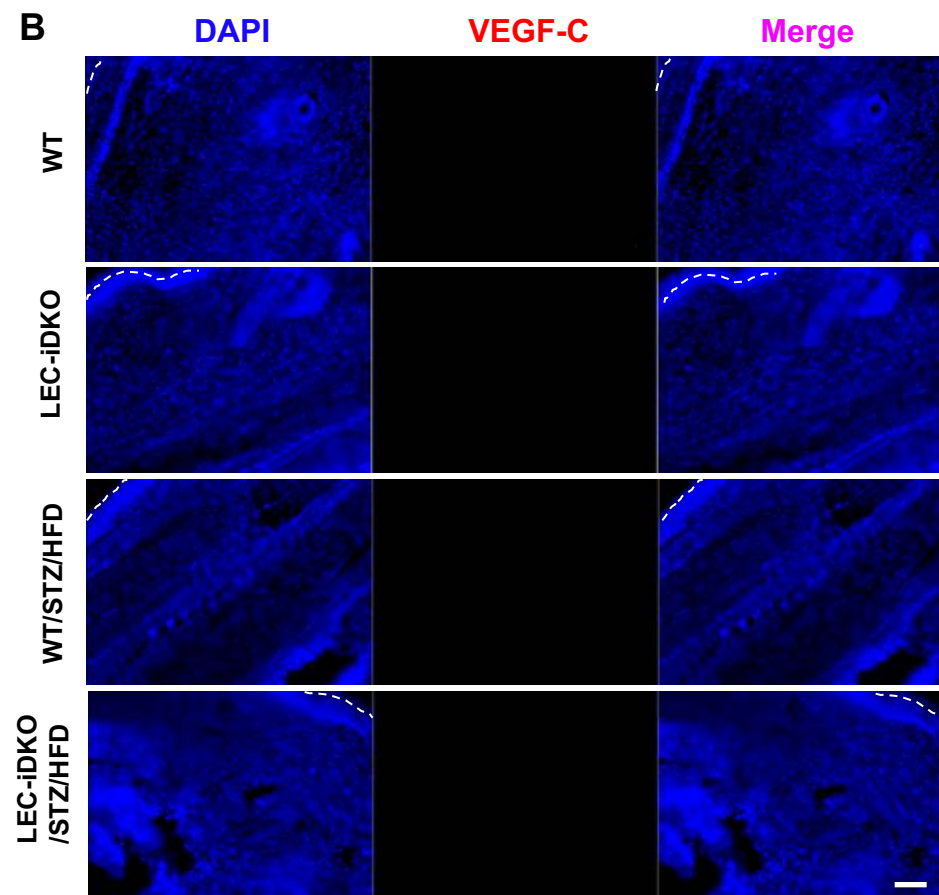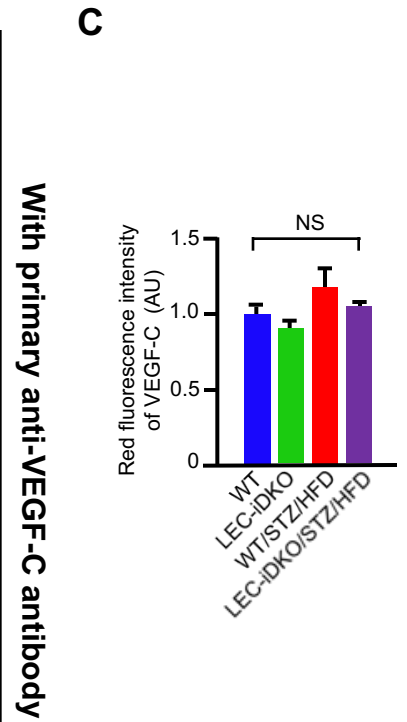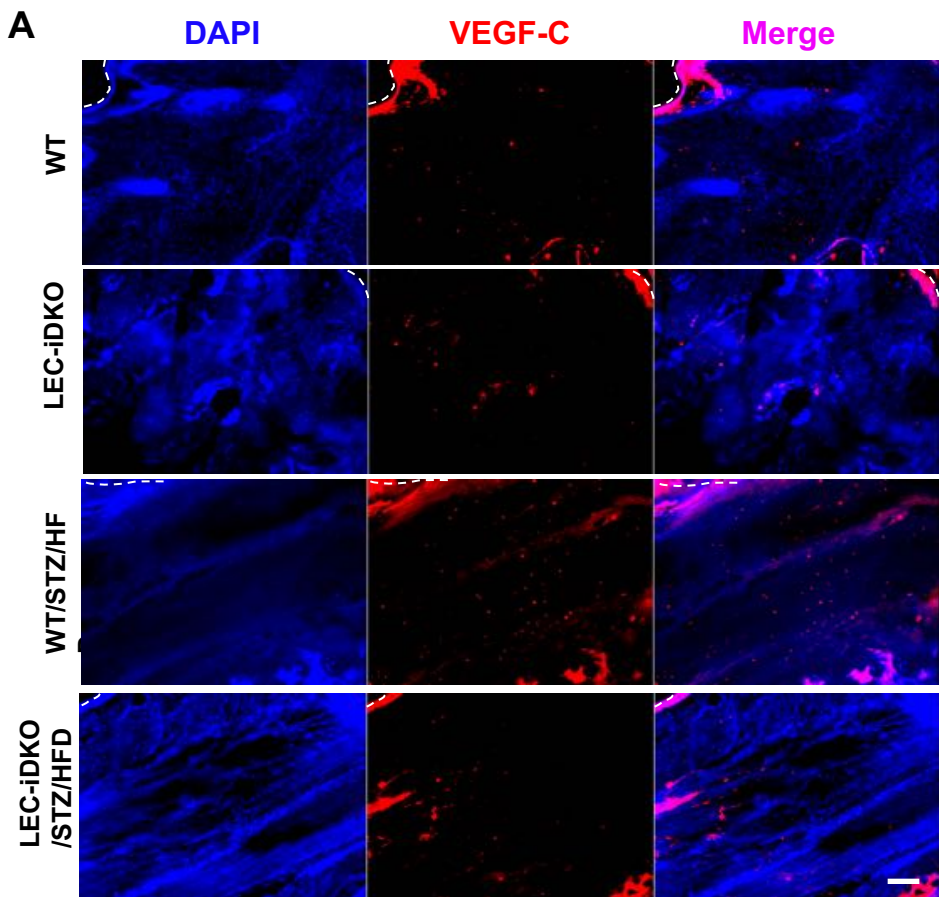
Supplemental Figure 11 (Related Figure 7). VEGF-C levels in tail edema tissue and serum from WT, LEC-iDKO, WT/STZ/HFD, and LEC-iDKO/STZ/HFD mice. (**A**) Representative images of VEGF-C levels measured in tail edema of WT, LEC-iDKO, WT/STZ/HFD, LEC-iDKO/STZ/HFD mice at postoperative Day 14 respectively (n=8). (**B**) Representative images of control staining without primary Rabbit anti-VEGF-C antibodies. (**C**) Quantifications of VEGF-C levels in mouse tail edema in **A,** by using Adobe Photoshop to calculate total number of pixels in red fluorescence (VEGF-C) using Adobe Photoshop's histogram tool on the DAPI blue channel. The red pixels of LEC-iDKO, WT/STZ/HFD, and LEC-iDKO/STZ/HFD were calculated by their ratios with WT images. All values are mean ± SD; n=5, ns: no statistics significance. Scale bar: 10 μm. (**D**) VEGF-C levels measured in serums from WT, LEC-iDKO, WT/STZ/HFD, and LEC-iDKO/STZ/HFD mice by Western Blot. (**E**) Quantification of VEGF-C levels in mouse serums in **D.** Quantifications by using NIH ImageJ, n=5. AU, Arbitrary Units. Data represent mean ± SEM, NS: not statistically significant by 2-way ANOVA.

Supplemental Figure 12

A

B
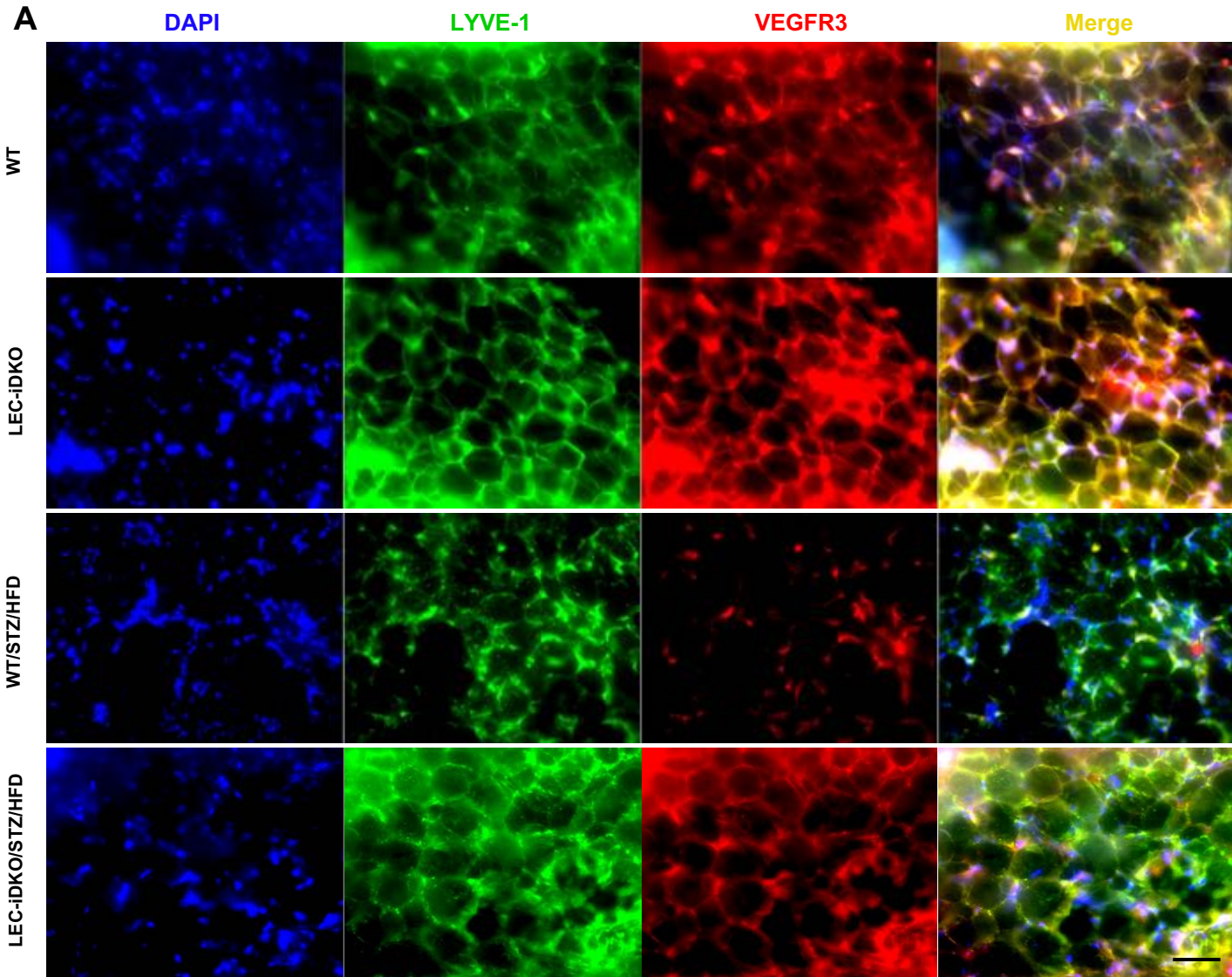
Supplemental Figure 12. Lymphatic formation in the skin from WT, LEC-iDKO, WT/STZ/HFD, and LEC-iDKO/STZ/HFD mice. (**A**) Representative images of lymphatic formation of skin stained with LYVE-1 (green) and VEGFR3 (red) of WT, LEC-iDKO, WT/STZ/HFD, LEC-iDKO/STZ/HFD mice. (**B**) Quantification of yellow fluorescence intensity in **A**. Quantifications by using NIH ImageJ, n=5; data represent mean ± SEM, *$P < 0.05$, by 2-way ANOVA followed by Tukey's post hoc test.

Supplementary Figure 13

A WT

B LEC-iDKO

C WT/STZ/HFD

D LEC-iDKO/STZ/HFD

E Control

F
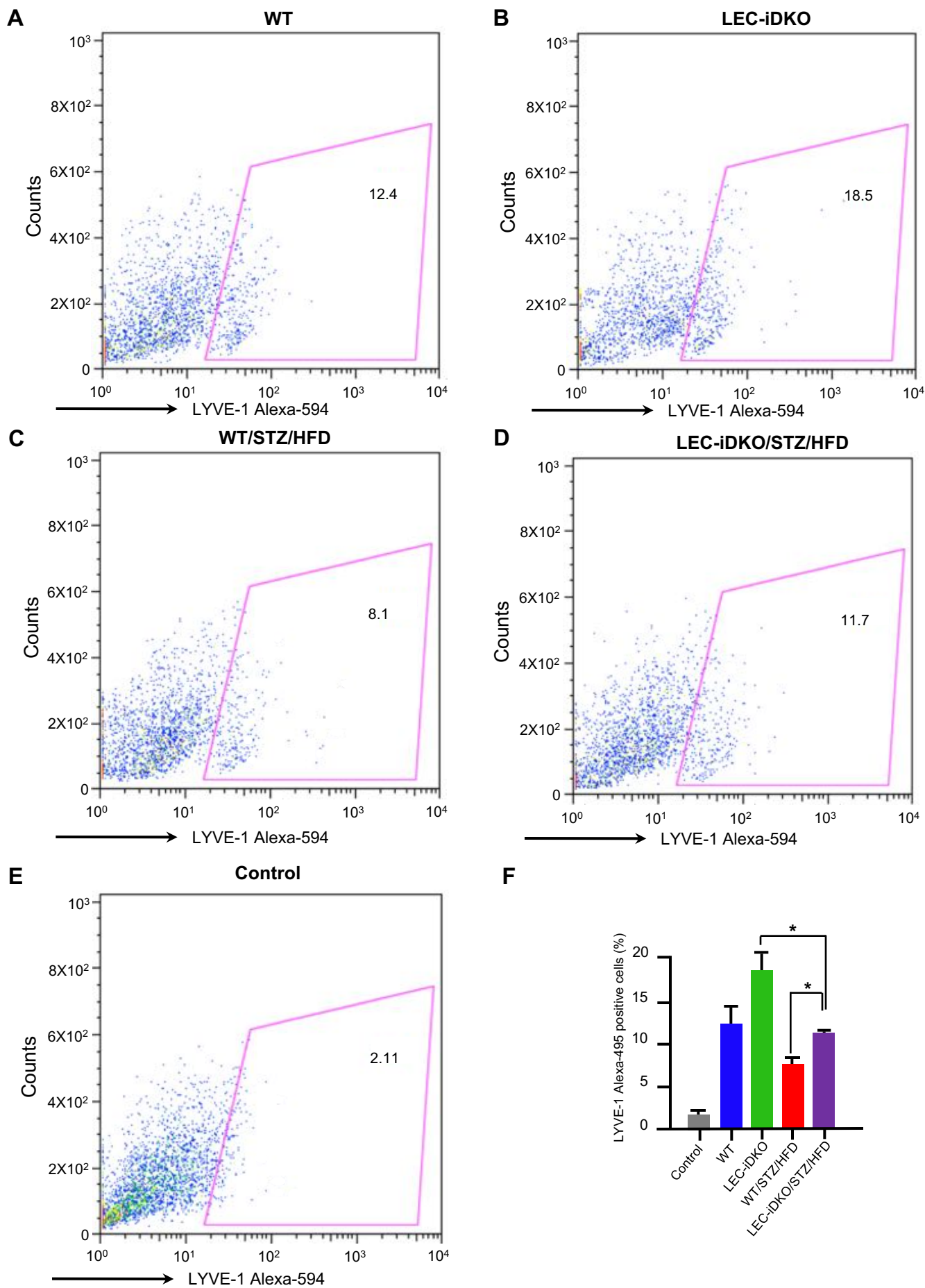
Supplemental Figure 13. Lymphangiogenesis in mouse skins. (A-E) Flow cytometric analysis showing the proportion of total LYVE-1$^+$ cells in WT (**A**), LEC-iDKO (**B**), WT/STZ/HFD (**C**), and LEC-iDKO/STZ/HFD (**D**) mouse skins. (**E**) Control: no LYVE-1$^+$ cells. (**F**) Quantifications of lymphangiogenesis in **A-D**. Data are representative of three independent experiments. Data represent mean ± SEM. n=5. *$P < 0.05$, by 2-way ANOVA followed by Tukey's post hoc test.

Supplemental Figure 14

A

B

Day 14

C

D
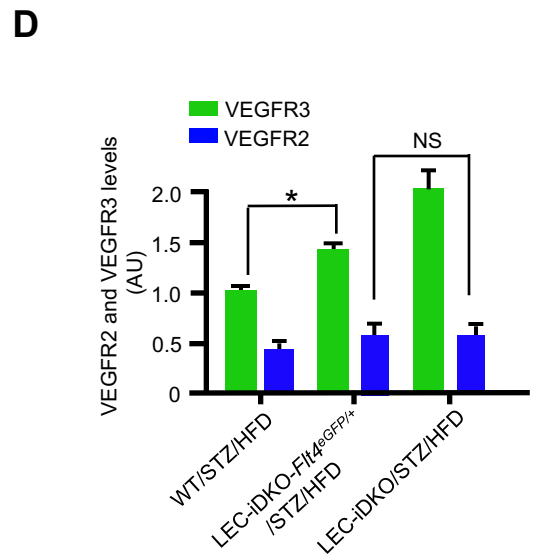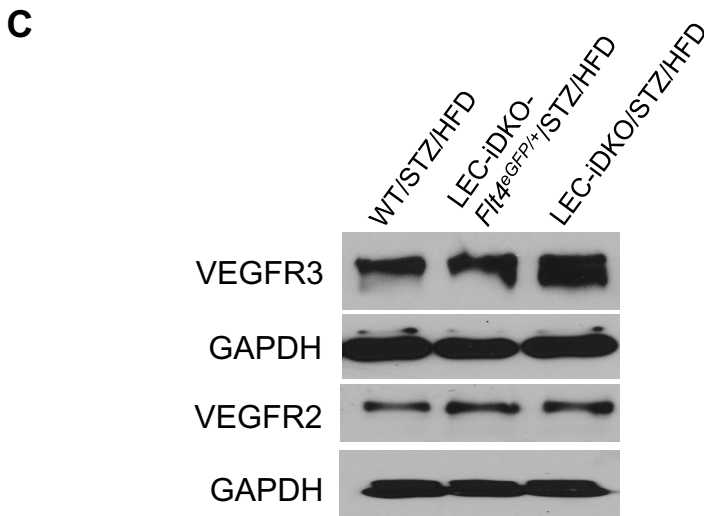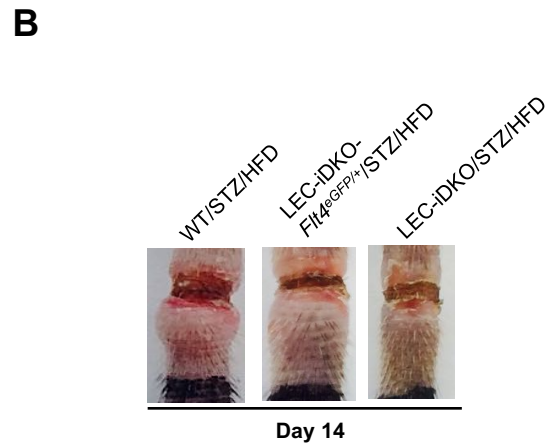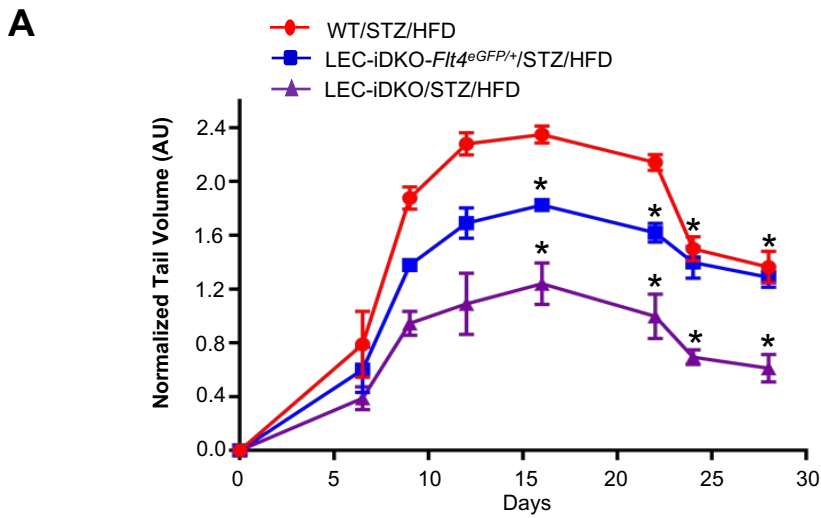
Supplemental Figure 14. VEGFR3 heterozygote on an inducible LEC-iDKO background (LEC-iDKO-*Flt4*eGFP/+) shows exaggerated secondary lymphedema. (**A**) Quantification of tail volume distal to the incision of postoperative tail edema of WT/STZ/HFD (n=8), LEC-iDKO-*Flt4*eGFP/+/STZ/HFD (n=8), and LEC-iDKO/STZ/HFD (n=8) mice at postoperative Days 1, 7, 9, 12, 17, 22, 24, and 28 respectively. (**B**) Representative images of postoperative tail edema of WT/STZ/HFD (n=8), LEC-iDKO-*Flt4*eGFP/+/STZ/HFD (n=8), and LEC-iDKO/STZ/HFD (n=8) mice at postoperative Day 14. (**C**) Western blot analysis for the VEGFR2 and VEGFR3 levels in LECs from WT/STZ/HFD, LEC-iDKO-*Flt4*eGFP/+/STZ/HFD, and LEC-iDKO/STZ/HFD mice. (**D**) Quantifications in **C** by using NIH ImageJ, n=5. Data represent mean ± SEM. AU, Arbitrary Units, NS: not statistically significant. *$P < 0.05$, by 1-way ANOVA followed by Tukey's post hoc test.

Supplemental Figure 15
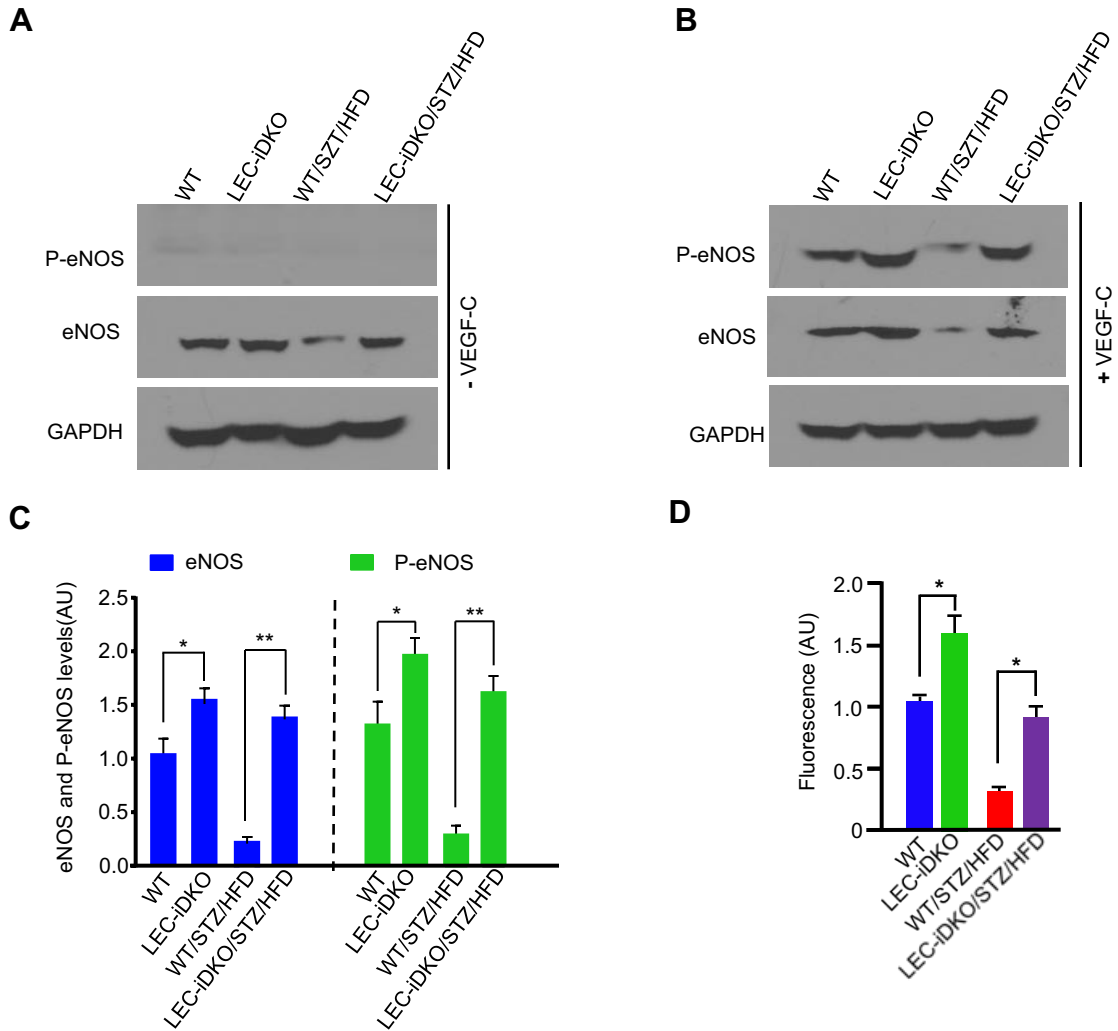
Supplemental Figure 15. (**A-B**) LEC cells were cultured in EC medium supplemented with 5µm 4-hydroxytamoxifen for 4 days. Cells were starved in F12K/DMEM medium (1:1) overnight and stimulated with VEGFC (100 ng/ml) for 30 min. Cell lysates were subjected to western blot analysis for eNOS and phosphor-eNOS. (**C**) Quantifications of levels of eNOS (blue, the left panel) or phosphor-eNOS (green, the right panel) in **A** and **B** respectively. (**D**) The NO production levels in LECs from WT, LEC-iDKO, WT/STZ/HFD, and LEC-iDKO/STZ/HFD mice were determined by the fluorescent indicator DAF-2. Quantifications of western blot bands by using NIH ImageJ, n=5. Data represent mean ± SEM. AU, Arbitrary Units. *$P < 0.05$; **$P < 0.01$, by 2-way ANOVA followed by Tukey's post hoc test.

Supplemental Figure 16
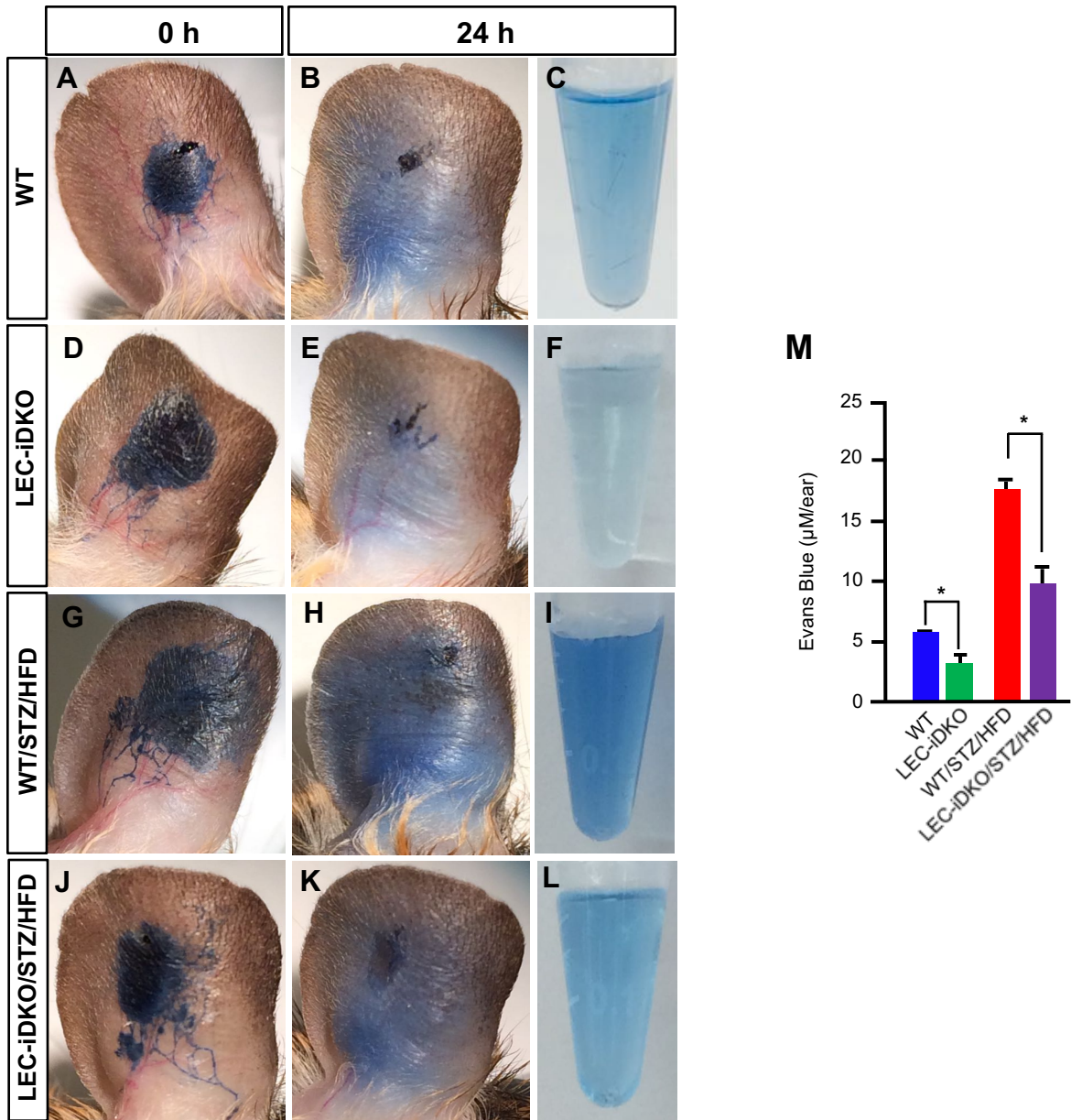
Supplemental Figure 16. Epsin deficiency promotes lymph flow under diabetic condition. (A-M) Evans blue visual lymphangiography and subsequent quantification was performed to follow lymph drainage patterns. Evans blue injection into the dermis of the ears of WT, LEC-iDKO, WT/STZ/HFD, and LEC-iDKO/STZ/HFD mice. (**M**) Extravasation of Evans blue dye after 24 hours were measured in ear skin. Plot shows mean ± SEM. n = 5. *$P < 0.05$, by 2-way ANOVA followed by Tukey's post hoc test.